O. J. Maselli, N. J. Chellman, M. Grieman, L. Layman, J. R. McConnell, D. Pasteris, R. H. Rhodes, E. Saltzman, and M. Sigl

Sea ice and pollution-modulated changes in Greenland ice core methanesulfonate and bromine

Climate of the Past, 2016; Online Publ:1-39

Clim. Past Discuss., doi:10.5194/cp-2016-49, 2016
Manuscript under review for journal Clim. Past
Published: 10 May 2016

Climate of the Past
Discussions
Open Access
EGU

Sea ice and pollution-modulated changes in Greenland ice core methanesulfonate and bromine

O.J. Maselli[1*], N.J. Chellman[1], M. Grieman[2], L. Layman[1], J. R. McConnell[1], D. Pasteris[1], R.H. Rhodes[3], E. Saltzman[2], M. Sigl[1]

[1] {Desert Research Institute, Department of Hydrologic Sciences, Reno, NV, USA}

[2] {University of California Irvine, Department of Earth System Science, Irvine, CA, USA}

[3] {University of Cambridge, Department of Earth Sciences, Cambridge, UK}

[*] {now at: The University of Adelaide, Australia, 5000}

Correspondence to: Olivia Maselli (olivia.maselli@adelaide.edu.au)

Keywords: bromine, MSA, nitrate, sea ice, pollution, acidification, Arctic, Greenland, cryosphere

Clim. Past Discuss., doi:10.5194/cp-2016-49, 2016
Manuscript under review for journal Clim. Past
Published: 10 May 2016

Climate of the Past Discussions
Open Access
EGU

Abstract

Reconstruction of past changes in Arctic sea ice extent may be critical for understanding its future evolution. Methanesulphonate (MSA) and bromine concentrations preserved in ice cores have both been proposed as indicators of past sea ice conditions. In this study, two ice cores from central and NE Greenland were analysed at sub-annual resolution for MSA (CH_3SO_3H) and bromine, covering the time period 1750-2010. We examine correlations between ice core MSA and the HadISST1 ICE sea ice dataset and consult back-trajectories to infer the likely source regions. A strong correlation between the low frequency MSA and bromine records during preindustrial times indicates that both chemical species are likely linked to processes occurring on or near sea ice in the same source regions. The positive correlation between ice core MSA and bromine persists until the mid-20th century, when the acidity of Greenland ice begins to increase markedly due to increased fossil fuel emissions. After that time, MSA levels decrease as a result of declining sea ice extent but bromine levels increase. We consider several possible explanations and ultimately suggest that increased acidity, specifically nitric acid, of snow on sea ice stimulates the release of reactive Br from sea ice, resulting in increased transport and deposition on the Greenland ice sheet.

Clim. Past Discuss., doi:10.5194/cp-2016-49, 2016
Manuscript under review for journal Clim. Past
Published: 10 May 2016

Climate of the Past Discussions
Open Access
EGU

28

29 1 Introduction

30 Atmospheric chemistry in the polar regions is strongly modulated by physical, chemical, and biological
31 processes occurring in and around sea ice. These include sea salt aerosol generation, biogenic emissions
32 of sulphur-containing gases and halogenated organics, and the photochemical/heterogeneous reactions
33 leading to release of volatile, reactive bromine species. The resulting chemical signals influence the
34 chemistry of the aerosol deposited on polar ice sheets. For this reason ice core measurements of sea salt
35 ions, methanesulphonate (MSA), and bromine have been examined as potential tracers for sea ice extent
36 (Abram et al., 2013; Spolaor et al., 2013b, 2016; Wolff et al., 2003). The interpretation of such tracers
37 is complicated by the fact that their source functions reflect changes in highly complex systems, and
38 signals are further modified by patterns of atmospheric transport and deposition.

39 MSA is produced by the atmospheric oxidation of DMS ($(CH_3)_2S$). DMS is produced throughout the
40 world's oceans as a breakdown product of the algal metabolite DMSP, ($(CH_3)_2S^+CH_2CH_2COO^-$).
41 DMS emissions are particularly strong in marginal sea ice zones (Sharma et al., 2012), and this source
42 is believed to be a dominant contributor to the MSA signal in polar ice (Curran and Jones, 2000). Ice
43 core MSA records have been used extensively in Antarctica as a proxy for local sea ice dynamics.
44 Although the specifics of the relationship are highly site-dependent (Abram et al., 2013; Curran et al.,
45 2003) MSA has been proven to be a reasonably good proxy for sea ice conditions (e.g., (Curran and
46 Jones, 2000)). In the Arctic, the relationship between MSA and sea ice conditions is less straightforward
47 due to the likelihood of multiple source regions with different sea ice conditions contributing to the ice
48 core archived MSA (Abram et al., 2013). Until now, a significant, but rather weak (r =-0.37)
49 relationship between ice core MSA and Arctic sea ice has only been established for a record from a
50 Svalbard ice core (O'Dwyer et al., 2000). In this study we analyse the direct correlations between the
51 MSA records from two Greenland ice core sites and the surrounding sea ice conditions in order to
52 demonstrate the utility of MSA as a local sea ice proxy.

53 In this study, all dissolved or suspended bromine species are measured (including organic bromine) and
54 shall be referred to as "bromine". The primary source of total inorganic bromine (e.g. Br_2, Br^-, HBr)
55 in the marine boundary layer (MBL) is the ocean (Parrella et al., 2012; Sander et al., 2003). At
56 concentrations of less than 0.2% that of sodium (Na), bromide (Br^-) makes a small contribution to
57 ocean salinity. Br^- can be concentrated in the high latitude oceans when the sea water is frozen, since
58 the formation of the ice matrix exudes the sea-salts in the form of brine (Abbatt et al., 2012). Small, sea-
59 salt aerosol particles blown from the surface of sea ice are typically enriched with bromine (Sander et
60 al., 2003) and satellite imagery has revealed that plumes of bromine (as BrO) are photo-chemically

Clim. Past Discuss., doi:10.5194/cp-2016-49, 2016
Manuscript under review for journal Clim. Past
Published: 10 May 2016

released from sea-ice zones in spring (Nghiem et al., 2012; Schönhardt et al., 2012; Wagner et al., 2001). Recently, studies have begun to link ice core records of bromide enrichment (relative to sea water Na concentrations) preserved in polar ice sheets to that of local sea ice conditions (Spolaor et al., 2013a, 2013b, 2014). Spolaor and co-workers demonstrated the spring-time Br^{-}/Na that is preserved in the ice core is a record of bromine explosion events over adjacent seasonal sea ice. A Br^{-}/Na enrichment would therefore indicate a larger seasonal sea ice extent or conversely a shorter distance between the ice edge and the ice core site due to decreased multi-year sea ice (Spolaor et al., 2013a). However, like MSA, it is likely that the bromine – sea-ice relationship in the Arctic is complicated by the myriad of bromine source regions which influence an ice core record in addition to factors which influence the degree of enrichment of the aerosol as it travels to the ice core site. In this study we compare ice core records of bromine to those of MSA and other common MBL species in order to determine the influence of sea ice conditions and other factors on bromine concentrations.

Here we present measurements of MSA, bromine, and elemental tracers of sea salt and crustal input in two Greenland ice cores covering the time period 1750-2010 C.E.. These ice core records represent the first continuous, sub-annual resolution records of bromine in polar ice to extend beyond the satellite era. We examine the relationship between these two sea ice-modulated tracers, their relationship to independent historical estimates of sea ice distribution, and the influence of industrialization on atmospheric and ice core chemistry.

2 Methods

2.1 Ice cores

The 87 m 'Summit-2010' ice core was collected in 2010 close to Summit Station, Greenland (72°20'N 38°17'24"W). The average snow accumulation at Summit is ~0.22 m yr^{-1} water equivalent, with few instances of melt. Due to the relatively high snow accumulation rate, seasonal analysis of the sea salt species concentrations was feasible. The 213 m Tunu core was collected in 2013 (78° 2' 5.5"N, 33° 52' 48"W), approximately 3 km east of the Tunu-N automatic weather station, part of the Greenland Climate Network. The average snow accumulation at Tunu is ~0.11 m yr^{-1} water equivalent. The Summit-2010 and Tunu cores were dated using well-known volcanic horizons in sulfur (S). The dating of Summit-2010 was refined by annual layer counting using seasonal cycles in the ratio of non-sea salt S/Na (Sigl et al., 2015).

Clim. Past Discuss., doi:10.5194/cp-2016-49, 2016
Manuscript under review for journal Clim. Past
Published: 10 May 2016

Climate of the Past Discussions
Open Access
EGU

2.2 Sampling and analysis

The ice cores were sampled from 33x33 mm cross-section sticks using a continuous melter system (McConnell et al., 2002). The silicon carbide melter plate provides three streams from concentric square regions of the ice core sample: an innermost stream (with a cross sectional area of 144 mm^2), an intermediate stream (340 mm^2) and an outer stream that was discarded along with any contaminants obtained from handling of the ice core. The innermost melt stream was directed to two inductively coupled plasma-mass spectrometers (ICP-MS, Thermo Element II high resolution with PFA-ST concentric Teflon nebulizer (ESI)) run in parallel. All calibrations and runtime standards were run on both instruments and several elements were also measured in duplicate (Na, Ce, Pb) to ensure tracking between both ICP-MS. In addition, an internal standard of yttrium flowed through the entire analytical system and was used to observe any change in system sensitivity. The instrument measuring bromine was run at low resolution to get the highest sensitivity and there were no mass interferences observed at the bromine isotope mass monitored (79 amu). The sample stream was acidified to 1% HNO_3 to prevent loss of less soluble species, degassed just prior to analysis to minimize mixing in the sample line and sampled at a rate of 0.45ml min^{-1} (McConnell et al., 2002; Sigl et al., 2013). The following elements were measured by ICP-MS: Br, Cl, Na, Ca, S, Ce, and Pb. Calibration of the ICP-MS was based on a series of 7 mixed standards measured at the start and end of each day for all elements except for the halides. Due to the high volatility of acid halides, a set of 4 bromine and chlorine standards were made individually in a 1% UHP HNO_3 matrix from fresh, non-acidified intermediate stock solution (Inorganic Ventures) every day. The intermediate melt stream was directed to a continuous flow analysis (CFA) system on which nitrate ion (NO_3^-) and snow acidity (sum of soluble acidic species) were measured using the technique described by Pasteris (2012) in addition to other atmospheric species of interest (Röthlisberger et al., 2000).

A portion of the debubbled CFA melt stream (150 µl min^{-1}) was subsampled using a peristaltic pump for continuous on-line analysis of methanesulfonate by electrospray triple-quad mass spectrometer (ESI/MS/MS; Thermo-Finnigan Quantum). This subsample was mixed with pure methanol (50 µl min^{-1}) delivered using an M6 pump (VICI). The methanol was spiked with an internal standard of deuterated MSA ($CD_3SO_3^-$; Cambridge Isotopes) at a concentration of 52 nM. The isotope standard was calibrated against non-deuterated MSA standards prepared in water from non-deuterated MSA ($CH_3SO_3^-$; Sigma Aldrich). MSA was detected in negative ion mode using the $CH_3SO_3^-/SO_3^-$ transition (m/z 95/80) and $CD_3SO_3^-/SO_3^-$ (m/z 98/80). The concentration of MSA in the sample flow was determined from the ratio of the non-deuterated and deuterated signals after minor blank corrections. The analysis of MSA by batch analysis using ESI/MS/MS has been reported previously (Saltzman et al., 2006). This study is

Clim. Past Discuss., doi:10.5194/cp-2016-49, 2016
Manuscript under review for journal Clim. Past
Published: 10 May 2016

the first use of the technique for ice core MSA analysis in a continuous, on-line mode. The uncertainty in the MSA intensity as calculated from the standard calibrations is 1%.

2.3 Calculation of anthropogenic Pb, non sea-salt S, and Br enrichment

The Pb derived from anthropogenic sources (exPb) was calculated as the difference between total lead and that from dust sources:

$$\mathbf{exPb} = [\mathbf{Pb}]_{\mathbf{obs}} - [\mathbf{Ce}]_{obs} \times \left(\frac{[\mathbf{Pb}]}{[\mathbf{Ce}]}\right)_{\mathbf{dust}} \quad (1)$$

Where the $([\mathrm{Pb}]/[\mathrm{Ce}])_{\mathrm{dust}}$ mass ratio has the constant value of 0.20588 (Bowen, 1979).

Similarly the amount of non-sea salt sulphur (nssS) was calculated relative to the sea-salt sodium, ssNa:

$$\mathbf{nssS} = [\mathbf{S}]_{\mathbf{obs}} - [\mathbf{ssNa}] \times \left(\frac{[\mathbf{SO_4^{2-}}]}{[\mathbf{Na}]}\right)_{\mathbf{seawater}} \quad (2)$$

Where the $\left(\frac{[\mathrm{SO_4^{2-}}]}{[\mathrm{Na}]}\right)_{\mathbf{seawater}}$ mass ratio has the constant value of 0.252 (Millero, 1974). ssNa was calculated by comparison with calcium as both have sea salt and dust origins (Röthlisberger et al., 2002):

$$\boldsymbol{ssNa} = \frac{[\boldsymbol{Na_{obs}} \times \boldsymbol{R_t} - \boldsymbol{Ca_{obs}}]}{[\boldsymbol{R_t} - \boldsymbol{R_m}]} \quad (3)$$

Where R_t and R_m are the Ca/Na mean crustal and mean marine mass ratios of 1.78 and 0.038, respectively, (Millero, 1974).

Bromine enrichment factors relative to sea water concentrations were calculated using the following:

$$\boldsymbol{Br_{enrich}} = \left(\frac{[\mathbf{Br}]}{[\mathbf{Na}]}\right)_{\mathbf{obs}} \Big/ \left(\frac{[\mathbf{Br}]}{[\mathbf{Na}]}\right)_{\mathbf{seawater}} \quad (4)$$

where the $([\mathrm{Br}]/[\mathrm{Na}])_{\mathrm{seawater}}$ mass ratio is 0.00623 (Millero, 1974).

Clim. Past Discuss., doi:10.5194/cp-2016-49, 2016
Manuscript under review for journal Clim. Past
Published: 10 May 2016

2.4 Air mass- back trajectories

To identify the likely sea ice source regions of MSA and Br deposited at the ice core sites, we perform 10 day air-mass back trajectories of boundary layer air masses from each ice core site using the GDAS1 archive dataset in the Hysplit4 software (Draxler and Hess, 1998). The starting height of the back trajectories was 500 m to ensure that the monitored air masses travelled close enough to the surface at the ice core site to potentially deposit aerosols. The vertical velocity field was taken from the meteorological data files. Air mass back trajectories were started every 12 hours and allowed to travel for 10 days (total number of trajectories hours = 14400 hours per month). The number of hours that the trajectories spent in a 2°x2° degree grid was summed over all of the trajectories for that month between the years 2005-2013. Previous work showed that the rapid advection of MBL air was the likely source of reactive halogens at Summit (Sjostedt et al., 2007).

2.5 Sea Ice Correlation mapping

In order to assess the relationships between sea ice conditions and ice core chemistry, correlation maps were generated between annual MSA concentrations and monthly sea ice using the HadISST1 ICE dataset at 1° latitude-longitude monthly resolution (Rayner, 2003). Pre-1979 sea ice datasets were interpolated from sea ice extent maps compiled by Walsh (1978) which incorporate a variety of empirical observations. The data were later bias corrected using modern satellite data (Rayner, 2003). Correlations were performed separately for the satellite period (1979-2012) and for the extended record (1900-2012), excluding the period 1940-1952 when the record has no variability due to scarcity of data (Rayner, 2003). Because strong DMS emissions occur in marginal sea ice zones (Sharma et al., 2012), we considered both sea ice concentration (SIC) and the area of open water in the sea ice pack (OWIP) which represents the size of the marginal sea ice zone. OWIP is defined as the difference between sea ice area (calculated from sea ice concentration over the area of the grid cell) and sea ice extent (NSIDC). A SIC of 15% was used as the threshold for a grid cell to contribute to sea ice extent. The area of OWIP was calculated within the coastal areas as defined by the results of the air-mass back trajectories (Sect. 3.4).

Correlations were performed on an annual rather than seasonal basis because the seasonality of ice core MSA is distorted due to post depositional migration of MSA signal at depth in the snow pack (Mulvaney et al., 1992) (Fig. 3, S3). Outliers were removed from the MSA time series (see Fig. 2) before the correlations were performed using the technique described by Sigl (2013) for identifying volcanic signals using a 25 year running average filter.

Clim. Past Discuss., doi:10.5194/cp-2016-49, 2016
Manuscript under review for journal Clim. Past
Published: 10 May 2016

177 ## 3 Results

178 ### 3.1 Bromine

179 Ice core measurements of bromine at Summit and Tunu covering the period 1750-2010 are shown in
180 Fig. 2. Ice core Br levels at each site were stable until ~1830 when they decreased by ~1 nM,
181 establishing a new baseline that was stable until the early 1900s. Both ice cores also show a Br peak in
182 the late 20th century. A summary of the timing of inflections and concentrations can be found Table S1.

183 Sea-salt transport onto the Greenland ice sheet occurs predominantly during winter. Historically the
184 winter-time sea-salt maximum was believed to be due to increased cyclonic activity over the open
185 oceans (Fischer and Wagenbach, 1996) though more contemporary studies show that blowing snow
186 from the surface of sea-ice may be a significant source (Rankin et al., 2002; Xu et al., 2013; Yang et al.,
187 2008, 2010). At Summit, a winter-time maximum is observed in the most abundant sea salts, Na and Cl
188 (Fig. 3). Bromine also shows a significant winter-time signal, however the annual maximum appears in
189 mid-summer - at concentrations ~70% above winter levels (Fig. 3a). Comparison with Br measured in
190 weekly surface snow samples collected from Summit (from 2007-2013; GEOSummit project) confirms
191 that this summer signal is real and not a result of post-depositional modification of seasonality of the
192 bromine signal (Fig. S1). The results from that study confirm that total Br concentrations peak in
193 summer on the ice sheet closely following the Br cycle observed in the Summit-2010 ice core. In
194 addition to the comparison with the Geosummmit data, in the ice cores studied here there are routinely
195 more than 10 measurements made within a yearly layer of snow giving confidence to the allocation of
196 a summer maximum in bromine at Summit. Analysis of the annual cycle of bromine in the Tunu ice
197 core also shows a summer maximum when averaged over the entire ice core time series but with
198 significantly larger error than observed at Summit. The timing of this peak suggests a predominant
199 summer source of bromine that dwarfs that from winter sea salt sources.

200 The shape of the annual bromine cycle does change slightly over the course of the Summit record (see
201 Fig. 3). Starting in the early 1900s the annual bromine cycle slowly becomes broader. A slight shift in
202 the maximum from a solely summer peak in the preindustrial era towards a broad summer-spring peak
203 by 1970 is observed (Fig. 3 lower plot). Comparison with the sea salt tracer, sodium, which does not
204 undergo the large temporal shift and broadening of its seasonal cycle shows that this change in bromine
205 seasonality is not linked to changes in production or transport of sea-salt aerosols or even dating
206 uncertainties in the ice core but perhaps the introduction of an additional, smaller bromine source in the
207 spring-time during the industrial era.

208 Both ice cores show a predominantly positive Br enrichment throughout the year (Fig S2) relative to

Clim. Past Discuss., doi:10.5194/cp-2016-49, 2016
Manuscript under review for journal Clim. Past
Published: 10 May 2016

Climate of the Past Discussions
Open Access
EGU

both sea salt elements chlorine and sodium. This enrichment reaches a maximum in mid to late summer at Summit (Fig 3). We assume that this enrichment reflects Br enrichment in the aerosol transporting Br to the ice sheet. However, post-depositional reduction of the bromine concentration is a possibility during the summer months due to photolytic processes at the snow surface. This may be the cause of the noisiness of the bromine signal within the lower accumulation, Tunu core. However, the increased snow accumulation that occurs during the summer months in both central and northern Greenland (Chen et al., 1997) should act minimise these bromine depleting effects driven by increased insolation in summer.

A summer time maximum in Br enrichment was also observed by Spolaor (2014) in a short segments of Antarctic Law Dome ice core as well as two Arctic ice cores. Spolaor et al. believe that the main source of the inorganic bromine originated from spring-time bromine explosion events above sea ice and the summertime maximum could possibly be an indication of lag-time between bromine containing particles becoming airborne and their deposition. Further investigation is needed to definitively establish the seasonality of bromine deposition at the poles. However the results of the Arctic ice cores studied here suggest that the summer maximum in bromine deposition is indeed real.

In the Tunu ice core, 2% of the monthly bromine enrichment measurements (relative to Cl) were negative (less than the Br/Cl seawater ratio, Fig S2). In a comprehensive review of global aerosol Br measurements, Sander (2003) concluded that in general, aerosols which showed positive Br enrichment factors were of sub-micrometer size. These small aerosols can travel further (lifetimes of around 5-10 days) and due to their larger surface/volume ratio may experience more atmospheric processing than larger aerosols, resulting in the positive enrichment. It is possible that the negative enrichment values observed in the Tunu ice core are therefore a result of larger aerosols (> micrometer) reaching the site due to its proximity to the coast (and thus the likely sea ice aerosol source region) in comparison to Summit.

3.2 MSA

The Summit-2010 MSA record (Fig. 2) replicates that measured by Legrand in 1993 (Legrand et al., 1997) and extends it an additional 17 years. The Tunu measurements represent the first MSA profile at this location. At Summit, MSA concentrations averaged 48 nM in the late 18th century, compared with just 27 nM at Tunu. From 1878-1930 MSA concentrations at Summit plateaued at 36 nM after which they began to drop rapidly, at a rate of 0.27 nM/year, reaching 18 nM by 2000. Large fluctuations in the MSA record after this time make it difficult to assess the most recent trend in Summit MSA concentrations. MSA concentrations in the Tunu core showed a similar variability to those in the

Clim. Past Discuss., doi:10.5194/cp-2016-49, 2016
Manuscript under review for journal Clim. Past
Published: 10 May 2016

241 Summit record, and until the mid-20th century, were consistently lower in magnitude. MSA
242 concentrations only began to decline consistently at Tunu after 1984, almost 50 years after the rapid
243 decline observed in the Summit record. After 2000, large fluctuations in concentration were again
244 observed making the modern-day trend in MSA concentration at Tunu difficult to establish.

245 Comparison with the total sulfur record (Fig. 4) reveals that during the preindustrial period, MSA
246 contributes to ~12% and ~ 7% of the total sulfur signal at Summit and Tunu, respectively, compared
247 with < 2% at the height of industrial period (1970 C.E.) at both sites.

248 The low frequency, preindustrial trend in MSA concentrations seen in these ice core records closely
249 follows that of bromine; particularly distinct is the decrease in both MSA and bromine at both sites in
250 the early 1800s (Tables S1and S2). In the early 1900s, however, both sites show a divergence between
251 the MSA and Br records—as MSA begins to decline, Br concentrations increase.

252 A dramatic shift in the 'timing' of the annual MSA maximum in Summit-2010 ice core is illustrated in
253 Figs. 3c and S3. The signal shifts gradually and continuously along the length of the the entire Summit-
254 2010 record from a spring to winter maximum (Fig. S3). This phenomenon has previously been
255 observed in several Antarctic ice cores and has been attributed to post-depositional migration within the
256 ice due to salt gradients (Mulvaney et al., 1992; Weller, 2004).

257 ### 3.3 Acidic Species

258 In winter, with the collapse of the polar vortex, polluted air masses enter the Arctic region as the
259 phenomenon known as the Arctic haze (Barrie et al., 1981; Li and Barrie, 1993). SO_2 and NO_x from the
260 haze are deposited on the ice/snow and oxidised to sulphuric (H_2SO_4) and nitric acid (HNO_3). There are
261 also natural sources of SO_2 (biomass burning, volcanic eruptions, oceans (Li and Barrie, 1993;
262 McConnell et al., 2007; Sigl et al., 2013) and NO_x(microbial activity in soils, biomass burning, lightning
263 discharges (Vestreng et al., 2009) as well as other snow/ice acidifiers including MSA, hydrogen chloride
264 and organic acids released from biogenic or biomass burning sources (Pasteris et al., 2012).

265 Total snow acidity was stable at both sites from 1750 through to ~1900 except for sporadic, short-lived
266 spikes due to volcanic eruptions. The average preindustrial acidity was the same at both sites (~1.8 μM).
267 Both records also show two distinct maxima in acidity centred on 1920 and 1970 (Fig. 4) with Tunu
268 displaying higher acidity than Summit over the entire industrial period. Overlaid with the acidity is the
269 total sulphur (S) record for both ice cores. The high correlation between the acidity and S records
270 illustrates that the sulphur species are the dominant natural and anthropogenic acidic species in the ice
271 cores. The trend in acidity closely follows the global SO_2 emissions with maxima from coal (~1920)
272 and fossil fuel combustion (~1970), respectively (Smith et al., 2011). After 1970 the records of acidity

Clim. Past Discuss., doi:10.5194/cp-2016-49, 2016
Manuscript under review for journal Clim. Past
Published: 10 May 2016

and S deviate. This deviation can be attributed to the presence of nitric acid that remains at a relatively high concentration in the late 20th century whilst sulphur species reduce in concentration (Fig. 4).

NO_3^- concentrations show no trend during the preindustrial era in either ice core records, averaging 1.1(±0.02) μM and 1.3(±0.03) μM for Summit and Tunu, respectively. The higher signal-to-noise ratio in the Summit-2010 record reveals a small peak in NO_3^- concentrations centred on ~1910. The Tunu record also shows elevated NO_3^- concentrations over this period. However the large variability in the signal makes it difficult to establish a higher resolution temporal trend. Both records clearly show a large increase in NO_3^- after 1950, peaking in ~1990 and followed by a general decreasing trend with the average until 2010 C.E. NO_3^- levels still double that of preindustrial concentrations: 2.1μM and 2.3 μM at Summit and Tunu, respectively.

The nitrate records from both sites follow the trend in northern hemisphere NO_x emissions with a peak in ~1910 and 1990 C.E.– a result of emissions from increases in both Northern Hemisphere fertilizer usage and biomass and fossil fuel combustion (Felix and Elliott, 2013).

3.4 Air mass back trajectories

Air mass back trajectory results demonstrate that air masses reaching the Summit-2010 site between March and July originate primarily from the South/South-East of the ice core site (Fig. 5a). Previous back trajectory analyses by Kahl *et al*. (1997) also linked individual spikes in their Summit MSA record to air masses that had passed over this same region of coast (SE Greenland) within the previous 1-3 days.Similar back trajectories were calculated for Summit-2010 at heights of 500 and 10,000m (Fig. 5a, S4a) illustrating that air masses that travel in the free troposphere and lower troposphere follow similar back trajectories and likely share the same source regions.

The results for Tunu indicate that air masses arrive primarily from the west coast of Greenland, passing over the Baffin Bay area, but there is also significant contribution from both the SE and NE (in May) coastal areas (Fig. 6b, S4b). Of these two secondary areas it is likely that aerosols transported from the NE would have a greater influence on the ice core concentrations due to proximity to the ice core site. Aerosol deposited at Tunu therefore represents a mixture of source regions, but are likely dominated by the NW Greenland, Baffin Bay coastal region.

3.5 MSA - Sea Ice correlations

Locations which showed a sea ice concentration (SIC) variability greater than 10% (the average estimated range of uncertainty in the satellite measurements) and have a significant correlation to MSA (t-test, $p<0.05$) are displayed in Fig. 6 and 7. A greater weight must be placed on the post-1979 sea ice

Clim. Past Discuss., doi:10.5194/cp-2016-49, 2016
Manuscript under review for journal Clim. Past
Published: 10 May 2016

concentration maps (Fig. 6b, Fig. 7b) as these were derived from passive microwave satellite data and, where available, operational ice chart data. The likely air-mass source regions, as defined by the results of the air-mass back trajectories, are indicated by the black bordered regions in Figs. 6 and 7. Within these areas there is generally a negative correlation between SIC and MSA, particularly in the spring months. The large areas of positive correlation along the east coast and in the western Barents Sea are striking, however, these areas are outside of the defined air-mass source region and thus are unlikely to be contributing to the ice core aerosol records. The positive correlation is likely an artefact of the negative autocorrelation between sea ice conditions in this region and the SE coast source region (Fig. S5).

Over the period 1900-2010 C.E. highly significant correlation (t-test, $p<0.001$) is found between the annual ice core MSA and the amount of open water in the ice pack (OWIP, representing the area of the marginal sea ice zone, Fig. 6a, Fig. 7a) in these aerosol source areas. For both ice cores the source region OWIP is stable until ~1970, when it begins to decline; a trend followed by the MSA. Over the shorter, satellite era (1979–2010), both the Summit-2010 and Tunu sites show strongest correlation between annual MSA and OWIP in March – when the break-up of the winter sea ice begins ($r = 0.33$, $p< 0.1$; $r = 0.37$, $p<0.05$, Fig. 7b, Fig. 8b). The significance of the Tunu correlation over this period can be dramatically increased ($r = 0.58$; $p<0.001$), if the closer, secondary source region (NE Greenland) is assumed to also influence the site (not shown).

3.6 MSA and bromine relationship

In an era where climate is driven by only natural forcings, chemical species that share a common source should show broadly consistent variability. This is evident in the preindustrial section of both ice core records where the relationship between MSA and Br (monitored as Br/MSA) remains constant over the entire period (Fig. 4) despite individual records going through step function changes. Using a 25 year running average on all records, the correlation between MSA and Br over the preindustrial period was calculated as: Summit-2010: r=0.282 (p=0.0008); Tunu: r= 0.298 (p = 0.0004), n= 138. After ~1930, relative increases in Br concentrations cause the Br/MSA ratio to increase above the stable preindustrial levels by more than 160%, reaching a peak in ~2000 C.E. at both sites.

Bromine in excess of what is expected from a purely sea ice source (exBr) was calculated by comparison to the other sea ice proxy, MSA. A linear regression of Br versus MSA was performed with the preindustrial data to establish the relationship between the two proxies during an era free of anthropogenic forcing. This relationship was then extrapolated into the period after 1850 C.E. in order to estimate the amount of bromine sourced only from sea-ice sources during the industrial era. The MSA

Clim. Past Discuss., doi:10.5194/cp-2016-49, 2016
Manuscript under review for journal Clim. Past
Published: 10 May 2016

record was smoothed with a 264 point Stineman function before being used in the extrapolation to reduce the noise in the resultant record whilst maintaining the low frequency trends. exBr is thus the difference between the total bromine measured and the calculated, natural sea ice bromine (in contrast to Br_{exc} defined by Spolaor (2016) as the amount of bromine in excess of the Br/Na seawater ratio).

An estimate of the amount of bromine measured in excess of what is expected from a purely sea ice source (exBr) is shown is Fig. 8. By definition, exBr is constant during the preindustrial period, but during the industrial period exBr peaks, reaching a broad maximum between 1980-2000 C.E. of ~2nM and 5nM at Summit and Tunu, respectively.

4 Discussion

The significant correlation between variability of marginal sea ice zone (OWIP) area within the identified source regions and the MSA records suggests that MSA records can be used as a proxy for modern sea ice conditions in these areas. Assuming that no major changes in atmospheric circulation patterns occurred to change the source regions for the marine aerosols between the preindustrial and industrial periods, our identification of MSA as a sea ice proxy (specifically a marginal sea ice zone proxy) may be valid for time periods both before and after 1850 at each ice core site. One major Northern Hemisphere climate phenomena is the North Atlantic Oscillation (NAO). NAO proxy records developed in Greenland ice core records (Appenzeller et al., 1998) suggest that although the NAO has shown variability over the past 200 years, its effect is damped in Northern Greenland (Appenzeller et al., 1998; Weißbach et al., 2015).

The MSA records reveal that after 1820 a gradual decline in sea ice occurred along the southern Greenland coast (reflected in the Summit-2010 core) and that this decline in sea ice did not extend significantly to the most northern Greenland coastline (reflected in the minimal change in Tunu MSA during this period). It is not unexpected that the Summit-2010 record would show the most dramatic changes in sea ice since we have demonstrated that the Summit sea ice proxy (MSA) is sourced from the south-east Greenland coast – an area sensitive to climate changes as it is primarily covered by young, fragile sea ice. The timing of the sea ice decline is coincident with the end of the Little Ice Age, identified from $\delta^{18}O$ ice core records as spanning the period 1420-1850 A.D. in Greenland (Weißbach et al., 2015). The dramatic dip in sea ice reflected in both the Tunu MSA and Br records at 1830 A.D. (and also seen less dramatically in Summit) also appears in the multi-proxy reconstruction of sea ice extent in the Western Nordic Seas performed by Macias Fauria et. al. (2010). This may be evidence of a sea ice decline event isolated to the east Greenland coast as the ice core records do not replicate the dramatic, early 20th century fluctuations observed in the latter part of the Western Nordic Seas reconstruction.

Clim. Past Discuss., doi:10.5194/cp-2016-49, 2016
Manuscript under review for journal Clim. Past
Published: 10 May 2016

From the ice core records it appears that the greatest decline in Greenland sea ice began in the mid 20th century, dropping to levels that are unprecedented in the last 200 years. This decline is observed along the entirety of the Greenland coast. Sea ice declined first around the southern coast (from 1930 A.D., reflected in Summit-2010) followed 54 years later by the more northern coastline (reflected in the Tunu record, see infection timings in Table S1). This sea ice decline is coincident with the sustained increase in greenhouse gases which has been identified as the major climate forcing and driver of increased global temperatures during the 20th century (Mann et al., 1998) and follows the same general trend in Arctic wide sea ice extent observed by Kinnard (2008).

Bromine has also been suggested as a possible proxy for sea ice conditions, however the timing of the largest bromine aerosol flux, in summer, does not coincide with the largest growth or extent of new sea ice. Sea ice begins to increase only at the end of summer as the fractures in the ice cover are re-laminated and the ice edge begins to advance southward (see Fig. 3f).

So what is the summer-time source of bromine? What is the cause of the increase in spring-time bromine explosion events in the industrial era? (see Fig. 3, lower panel) and why does the bromine record deviate from the sea ice proxy record (MSA) around the same time? Possible sources of bromine and the factors which may effect the resultant bromine flux are discussed below.

4.1 Alternate sources of bromine

4.1.1 Combustion of coal

Bromine is present in coal (Bowen, 1979; Sturges and Harrison, 1986) and coal burning is therefore a potential source of increased bromine deposition on the Greenland ice sheet over the period 1860-1940 (McConnell and Edwards, 2008). McConnell et al. (2008; 2007) demonstrated that pollution from the Northern American coal burning era was deposited all over Greenland leaving as its fingerprint large amounts of black carbon and toxic heavy metals. Sturges (1986) measured the relative concentrations of Br and Pb in particulates emitted from the stacks of coal fired power stations and found a molar ratio (Br:Pb) ranging between 0.36-0.67:1. Figure 8 illustrates that at both Summit and Tunu the exPb (lead not from dust sources) preserved in the ice cores over the coal burning era was less than 1nM. This concentration implies that the upper limit to the amount of bromine deposited from coal combustion would be 0.67nM (assuming no loss of bromine from the particulates during transportation). This is an insignificant amount compared to the total Br signal preserved in the ice at this time. Coal combustion is not the major cause of the elevated industrial Br concentration.

Clim. Past Discuss., doi:10.5194/cp-2016-49, 2016
Manuscript under review for journal Clim. Past
Published: 10 May 2016

398 #### 4.1.2 Leaded Gasoline

399 The largest historical, anthropogenic source of bromine is thought to be the combustion of leaded
400 gasoline. Large quantities of 1,2, diethyl bromide (DEB) were added to leaded fuel as a scavenger for
401 Pb preventing lead oxide deposition by converting it to volatile lead bromide salts as well as CH_3Br
402 (Oudijk, 2010;Nriagu, 1990;Berg et al., 1983). In 1925 gasoline had a Br:Pb molar ratio of 2:1 in a
403 formulation which is now called "aviation fluid'. The Br:Pb molar ratio was reduced to 1:1 in the 1940s
404 except in places such as the Soviet Union which continued to use "aviation fluid" for motor gasoline
405 (Thomas et al., 1997). Although the consumption of leaded gasoline has been well documented,
406 particularly in North America, the estimates of the emissions of bromine compounds from the
407 combustion process are still unclear. Estimates of the amount of DEB that is converted into gaseous
408 CH_3Br range from 0.1% to 25% (Bertram and Kolowich, 2000) and direct measurements of exhaust
409 fumes across NW England found a Br:Pb ratio of between (0.65-0.8):1 in the airborne particulates
410 (Sturges and Harrison, 1986).

411 The ratio of Br:Pb in the gasoline formulae can therefore be used only as an upper limit to predict the
412 Br:Pb ratio in gasoline combustion aerosols transported to the ice core sites. Figure 8 shows a
413 comparison between exBr and exPb measured in each ice core. Also illustrated is the upper limit of the
414 amount of bromine expected from gasoline sources assuming the 2:1 Br:Pb ratio for aviation gasoline
415 over the whole leaded gasoline era (blue) and just between 1925 and 1940 (green; representing source
416 regions outside the Soviet Union). World-wide leaded gasoline emissions were estimated to have peaked
417 in 1970 (Thomas et al., 1997)—an assumption that is supported by the observed timing of the exPb
418 maximum observed in both ice cores. Whilst it is likely that leaded fuel contributed to the increased
419 bromine observed between 1925 and 1970, it is clear that it was not the only contributor to the exBr
420 record, particularly after 1970 when the exBr record continues to rise despite a worldwide decline in
421 leaded fuel consumption. The disparity between the exPb and exBr records suggesting the driving force
422 for the enhanced emission of Br was still active and increasing after 1970.

423 #### 4.1.3 Seasonal salinity changes

424 Younger sea ice surfaces such as frost flowers, new and 1st year sea ice have a higher salinity and thus
425 have higher bromine concentrations than older sea ice surfaces (Hunke et al., 2011) . The salinity of sea
426 ice is at its maximum at the start of the winter season after which surface salinity slowly diminishes due
427 to gravitational draining (Hunke et al., 2011). As summer approaches, ice continues to undergo
428 desalination due to melting of surface snow which percolates through the ice (Hunke et al., 2011).
429 Satellite observations that the BrO flux from the sea ice declines over summer (despite increasing

Clim. Past Discuss., doi:10.5194/cp-2016-49, 2016
Manuscript under review for journal Clim. Past
Published: 10 May 2016

insolation) is likely due to the combined reduction in young sea ice area and in ice salinity. Ocean surface salinity decreases in the summer due to the increased meteoric water flux and melting of desalinated sea ice. Salinity increases are therefore unlikely to be the cause of the exBr flux observed in the ice core records and the observed summer maximum in bromine.

4.1.4 Organic bromine species

Gaseous bromocarbons can be a source of inorganic bromine to the snow pack when they react with •OH or to a lesser extent with $\bullet NO_x$ or by photolysis (Kerkweg et al., 2008; WMO, 1995) to form the less reactive, species HBr, $BrNO_3$ and $HOBr$. These species can then be washed out of the atmosphere and deposited on the snow surface due to their high solubility (Fan and Jacob, 1992; Sander et al., 1999; Yung et al., 1980).

The predominant source of gaseous bromine in the atmosphere is methyl bromide, CH_3Br (WMO, 2002). The major modern sources of CH_3Br are fumigation, biomass burning, leaded fuel combustion, coastal marshes, wetlands, rapeseed and the oceans (WMO, 2002). The ocean is also a major sink for CH_3Br, the temperature sensitive dissolution occurring through hydrolysis and chloride ion substitution to form bromide (WMO, 1995). ~30% of CH_3Br was from industrial emissions at the time of the global peak in the CH_3Br mixing ratio (1996-1998) (Montzka and Reimann, 2010). The timing of the massive increases in inorganic bromine seen at both ice cores sites coincides with the timing of maximum anthropogenic emissions of CH_3Br. However, the estimated 2.7 ppt increase in global tropospheric CH_3Br above preindustrial levels equates to only ~ 3.7 ppt (0.05nM) Br incorporated into the snow pack (assuming 100% conversion efficiency of CH_3Br in soluble Br species). This level is far less than the 2-5 nM increase in exBr observed in the ice cores during the industrial period.

Bromoform ($CHBr_3$) is emitted from vegetation such as marine phytoplankton and seaweed. It has the largest globe flux of all the bromocarbons (estimated at almost 5 times that of CH_3Br (Kerkweg et al., 2008). However, it is very short-lived (atmospheric lifetime of ~ 17 days (Ordóñez et al., 2012) and thus is confined to the marine boundary layer. Inorganic bromine formed from the destruction of $CHBr_3$ would therefore be representative of only local sources of organic bromine. The biological seasonal cycle maximises the production of $CHBr_3$ in summer and concentrations are greatly reduced but not negligible in winter (tidal forcing also influences bromocarbon emission by allowing coastal algae to dry-out (Kerkweg et al., 2008). The summer maximum in inorganic bromine at Summit (Fig. 3a) suggests that a biogenic source of bromine is dominant. However to-date biogenic sources have been considered insignificant in the Arctic marine boundary layer compared with the inorganic bromine source from sea salts (Simpson et al., 2007). These results suggest that a biogenic system should be

Clim. Past Discuss., doi:10.5194/cp-2016-49, 2016
Manuscript under review for journal Clim. Past
Published: 10 May 2016

reconsidered as a major source of the natural inorganic bromine flux to the polar regions.

4.2 Cause of the spring-time increase in bromine flux

4.2.1 Bromine explosion events

Spring is the time of 'bromine explosion' events above sea ice. Sea salt aerosols passing through these BrO plumes can become enriched with bromine by adsorbing the gaseous species (Fan and Jacob, 1992; Langendörfer et al., 1999; Lehrer et al., 1997; Moldanová and Ljungström, 2001; Sander et al., 2003). Nghiem (2012) showed that these bromine rich air masses can then be elevated above the planetary boundary layer and transported hundreds of kilometres inland. Increasing the frequency and duration of the bromine explosion events would therefore likely increase the amount of bromine delivered to the ice core sites during spring without influencing the total aerosol flux.

Spring-time field studies at Ny Ålesund, Svalbard have shown positive correlation between atmospheric filterable bromine species and elevated levels of sulphate and nitrate (Langendörfer et al., 1999; Lehrer et al., 1997) suggesting that acidic, anthropogenic pollution may be the driver of the observed increases in annual bromine enrichment during the industrial period.

4.2.2 Acidity effects on debromination

In remote, relatively clean environments such as the Arctic, even small increases in acidity are thought to affect the cycling of bromine in the snow pack (Finlayson-Pitts, 2003; Pratt et al., 2013; Sander et al., 1999). In the laboratory, increasing the acidity of frozen (Abbatt et al., 2010) and liquid salt solutions (Frinak and Abbatt, 2006; George and Anastasio, 2007) increased the yield of gas-phase Br_2 whilst at the same increasing the *solubility* of other bromine species, such as HBr. The uptake efficiency of HBr by acidic sulphate aerosols, for example, is estimated at 80% compared to 30% for sea salt aerosols (Parrella et al., 2012). Interestingly, Abbatt (1995) demonstrated that HBr is more than 100 times more soluble in super-cooled sulphuric acid solutions than HCl. This may explain the cause of bromine enrichment in the aerosol measured in the ice cores relative to the more abundant chlorine (Fig. S2). The results of both the laboratory and field studies suggest that increasing snow/ice acidity in the Arctic will likely enhance spring-time bromine explosion events above the sea ice whilst the increase in solubility allows the termination products of the explosion to be transported away from the sites on the surface of acidic aerosols. Increasing spring-time bromine aerosol concentrations would increase the average annual bromine concentrations deposited on the ice sheet and could explain the exBr records observed in both ice cores.

Clim. Past Discuss., doi:10.5194/cp-2016-49, 2016
Manuscript under review for journal Clim. Past
Published: 10 May 2016

Figure 9 illustrates that of the two dominant acidic species preserved in the ice, HNO_3 (represented by nitrate) shows the highest correlation to total bromine over sub-decadal time scales at both ice core sites. Records were detrended with an 11 year running average before comparison to isolate the high frequency components of each record. The bromine – sulfuric acid (represented by sulfate) correlation is not significant. This is primarily because there is no bromine response to the dominant volcanic sulphate spikes throughout the record. The large spikes in sulfate concentrations did not cause a depletion of bromine in the snowpack (Figure 9). This result might be expected if the increased acidity caused more bromine to volatize. These results suggest that HNO_3 is the most influential of the MBL acidic species in the processing and transport of Br on aerosols in the MBL.

4.2.3 NOx and links to bromine

The snow and atmospheric chemistries of bromine and nitrate (NO_3^-) are tightly linked. NO_3^- is one of the main sources of the •OH radical. The •OH radical can oxidize bromide salts and cause the release of gas-phase bromine species (Abbatt et al., 2010; Chu and Anastasio, 2005; George and Anastasio, 2007; Jacobi et al., 2014). Morin (2008) observed that the majority of nitrate that is deposited to the snow surface is of the form $BrNO_3$ in the coastal Arctic boundary layer. $BrNO_3$ forms by gas-phase reaction of BrO and NO_2. $BrNO_3$ is quickly adsorbed back onto the snow and aerosol surfaces due to its high solubility. The heterogeneous hydrolysis of $BrNO_3$ to again release bromine species back into the gas-phase has also been observed (Parrella et al., 2012) and can occur both during sunlight hours as well as in the dark (Sander et al., 1999). NO_x are intertwined with Br as it cycles between the gas and condensed phases.

The seasonality of the NO_3^- signal preserved in the ice cores is coherent with Br, showing a summer-time maximum (Fig. 3a,d). The slight shift in timing of the industrial nitrate seasonal maximum towards spring is replicated in the seasonal bromine signal preserved in the ice (Figure 3). The high correlation between the preindustrial (1750-1850) NO_3^- and Br records (Fig. 9) supports this observation of co-transport and sink of Br and NO_3^- into the snow pack, though the natural sources of each are distinctly different.

In the industrial era the low frequency temporal profile of the bromine (Fig. 2) and nitrate records (Fig. 4) differ dramatically, apparently questioning the tight relationship observed before 1850. However, the positive correlation between the nitrate and the Br/MSA records is striking at both sites. The large relative increase in bromine (compared with MSA) during the era of high NO_x pollution may point to a non-sea ice source of bromine linked to nitrate emissions.

Bromine and NO_x species shared a common source in the 20th century through the combustion of leaded

Clim. Past Discuss., doi:10.5194/cp-2016-49, 2016
Manuscript under review for journal Clim. Past
Published: 10 May 2016

524 gasoline (Sect. 4.1.2). As discussed above, we observe that leaded fuel pollution reaching the Arctic
525 began to decline after 1970 in-line with reduced global consumption, but the amount of bromine in-
526 excess of natural sources (exBr, Fig. 8) continued to increase – following the trends in NO_x pollution
527 (Fig. 4). The continued increase in NO_x despite the decline in leaded fuel combustion is attributed
528 primarily to biomass burning, soil emissions and unleaded fossil fuel combustion (Lamarque et al.,
529 2013). As the leaded fuel source of bromine began to decline, organic bromine pollutants continued to
530 increase, as was discussed in Sect. 4.1.4. This can only account for a small fraction of the observed Br.
531 The continued correlation between nitrate and exBr despite the decoupling of nitrate and bromine
532 anthropogenic sources after 1970, suggests that nitrate pollution is likely influencing the processing of
533 local, natural sources of bromine in the polar MBL, in effect increasing the mobility of the bromine and
534 thus its flux onto the ice sheet.

535 #### 4.2.4 Consequences of nitrate driven increased bromine mobility in the Arctic

536 Plumes of BrO emitted from sea ice regions have been linked to mercury deposition events which lead
537 to an increase in the bioavailability of toxic mercury species in polar waters (Parrella et al., 2012).
538 Increased spring-time mobilization of bromine from the sea ice induced by anthropogenic nitrate could
539 therefore increase the frequency and duration of these events and thus the mercury toxicity of the oceans.
540 Increased atmospheric bromine concentrations would also increase the frequency of ozone depletion
541 events (Simpson et al., 2007) thereby altering the oxidative chemistry of the polar MBL.

542 Whilst several studies have begun to explore bromine records from ice cores as a proxy for past sea ice
543 conditions, the results of this study demonstrate that in an era of massive increases in atmospheric acidity
544 the natural relationship between bromine and sea ice conditions can become distorted, precluding it
545 from being an effective modern-day Arctic sea ice proxy.

546

547 ## 5 Conclusion

548 In this study we have shown that high resolution MSA measurements preserved in ice cores can be used
549 as a proxy for sea ice conditions (specifically the size of the marginal sea ice zone) along specific
550 sections of the Greenland coast. The MSA records show that sea ice began to decline at the end of the
551 LIA and again, more dramatically during the Industrial period. Also, unsurprisingly, the changes in sea
552 ice conditions in the northern sites have been less dramatic than along the southern coastline.
553 Comparison between the 260 year records of bromine and MSA presented in this study allow us to show
554 that in the preindustrial era bromine concentrations preserved in the Greenland ice sheet are also likely
555 linked to the local sea ice conditions. With the decline of sea ice in the modern era and the dramatic

Clim. Past Discuss., doi:10.5194/cp-2016-49, 2016
Manuscript under review for journal Clim. Past
Published: 10 May 2016

increase in acidic pollutants reaching the Arctic the sea ice-bromine connection is distorted, precluding it from being an effective, direct sea ice proxy during the industrial era. The introduction of NO_x pollution in particular, into the clean Arctic environment promotes mobilization of bromine from the sea ice, which in turn increases the bromine enrichment of the sea salt aerosols, forcing more bromine inland (particularly in spring) than would occur naturally. Whilst Northern Hemisphere pollution may prevent bromine from being an effective modern-day sea ice proxy in the Arctic, in Antarctica the anthropogenic flux of nitrate species is thought to be small in comparison with natural sources (Wolff, 2013), leaving room for the possibility that bromine may still be an effective proxy for local Antarctic sea ice conditions.

Author contribution

Manuscript written and data analysis performed by O.J.M with expert editing by E.S.. Ice cores supplied by J.R.M.. Tunu ice core was collected and processed by O.J.M, J.R.M., N.J.C, M.S., R.H.R. under the leadership of Beth Bergeron. Ice cores dated by M.S., J.R.M.. ICP-MS and CFA measurements performed by O.J.M, J.R.M., N.J.C., L.L, D.P., M.S.. MSA measurements designed and performed by M.G., E.S.

Acknowledgements

This research was funded by the National Science Foundation; grant numbers 1023672 and 1204176.

Clim. Past Discuss., doi:10.5194/cp-2016-49, 2016
Manuscript under review for journal Clim. Past
Published: 10 May 2016

576 **References**

577 Abbatt, J., Oldridge, N., Symington, a, Chukalovskiy, V., McWhinney, R. D., Sjostedt, S. and Cox, R.
578 a: Release of gas-phase halogens by photolytic generation of OH in frozen halide-nitrate solutions: an
579 active halogen formation mechanism?, J. Phys. Chem. A, 114(23), 6527–33, doi:10.1021/jp102072t,
580 2010.

581 Abbatt, J. P. D.: Interactions of HBr, HCl, and HOBr With Supercooled Sulfuric- Acid-Solutions of
582 Stratospheric Composition, J. Geophys. Res., 100(D7), 14009–14017, 1995.

583 Abbatt, J. P. D., Thomas, J. L., Abrahamsson, K., Boxe, C., Granfors, A., Jones, A. E., King, M. D.,
584 Saiz-Lopez, A., Shepson, P. B., Sodeau, J., Toohey, D. W., Toubin, C., von Glasow, R., Wren, S. N.
585 and Yang, X.: Halogen activation via interactions with environmental ice and snow in the polar lower
586 troposphere and other regions, Atmos. Chem. Phys., 12(14), 6237–6271, doi:10.5194/acp-12-6237-
587 2012, 2012.

588 Abram, N. J., Wolff, E. W. and Curran, M. A. J.: A review of sea ice proxy information from polar ice
589 cores, Quat. Sci. Rev., 79, 168–183, doi:10.1016/j.quascirev.2013.01.011, 2013.

590 Appenzeller, C., Schwander, J., Sommer, S. and Stocker, T. F.: The North Atlantic Oscillation and its
591 imprint on precipitation and ice accumulation in Greenland, Geophys. Res. Lett., 25(11), 1939,
592 doi:10.1029/98GL01227, 1998.

593 Barrie, L. A., Hoff, R. M. and Daggupaty, S. M.: The influence of mid-latitudinal pollution sources on
594 haze in the Canadian arctic, Atmos. Environ., 15(8), 1407–1419, doi:10.1016/0004-6981(81)90347-4,
595 1981.

596 Bertram, F. J. and Kolowich, J. B.: A study of methyl bromide emissions from automobiles burning
597 leaded gasoline using standardized vehicle testing procedures, Geophys. Res. Lett., 27(9), 1423–1426,
598 doi:10.1029/1999GL011008, 2000.

599 Bowen, H. J. M.: Environmental chemistry of the elements / H. J. M. Bowen, Academic Press, London ;
600 New York., 1979.

601 Chen, Q. S., Bromwich, D. H. and Bai, L.: Precipitation over Greenland retrieved by a dynamic method
602 and its relation to cyclonic activity, J. Clim., 10(5), 839–870, 1997.

603 Chu, L. and Anastasio, C.: Formation of hydroxyl radical from the photolysis of frozen hydrogen
604 peroxide, J. Phys. Chem. A, 109(28), 6264–6271, doi:10.1021/jp051415f, 2005.

605 Curran, M. A. J. and Jones, G. B.: Dimethyl sulfide in the Southern Ocean: Seasonality and flux, J.
606 Geophys. Res., 105(D16), 20451, doi:10.1029/2000JD900176, 2000.

Curran, M. A. J., van Ommen, T. D., Morgan, V. I., Phillips, K. L. and Palmer, A. S.: Ice core evidence for Antarctic sea ice decline since the 1950s., Science, 302(5648), 1203–1206, doi:10.1126/science.1087888, 2003.

Draxler, R. R. and Hess, G. D.: An Overview of the HYSPLIT_4 Modelling System for Trajectories, Dispersion, and Deposition., Aust. Meteorol. Mag., 47(June 1997), 295–308, 1998.

Fan, S.-M. and Jacob, D. J.: Surface ozone depletion in Arctic spring sustained by bromine reactions on aerosols, Nature, 359(6395), 522–524, doi:10.1038/359522a0, 1992.

Felix, J. D. and Elliott, E. M.: The agricultural history of human-nitrogen interactions as recorded in ice core δ 15 N-NO3−, Geophys. Res. Lett., 40(8), 1642–1646, doi:10.1002/grl.50209, 2013.

Finlayson-Pitts, B. J.: The Tropospheric Chemistry of Sea Salt: A Molecular-Level View of the Chemistry of NaCl and NaBr, Chem. Rev., 103(12), 4801–4822, doi:10.1021/cr020653t, 2003.

Fischer, H. and Wagenbach, D.: Large-scale spatial trends in recent firn chemistry along an east-west transect through central Greenland, Atmos. Environ., 30(19), 3227–3238, doi:10.1016/1352-2310(96)00092-1, 1996.

Frinak, E. K. and Abbatt, J. P. D.: Br2 production from the heterogeneous reaction of gas-phase OH with aqueous salt solutions: Impacts of acidity, halide concentration, and organic surfactants., J. Phys. Chem. A, 110(35), 10456–64, doi:10.1021/jp063165o, 2006.

George, I. J. and Anastasio, C.: Release of gaseous bromine from the photolysis of nitrate and hydrogen peroxide in simulated sea-salt solutions, Atmos. Environ., 41(3), 543–553, doi:10.1016/j.atmosenv.2006.08.022, 2007.

Hunke, E. C., Notz, D., Turner, A. K. and Vancoppenolle, M.: The multiphase physics of sea ice: a review for model developers, Cryosph., 5(4), 989–1009, doi:10.5194/tc-5-989-2011, 2011.

Jacobi, H. W., Kleffmann, J., Villena, G., Wiesen, P., King, M., France, J., Anastasio, C. and Staebler, R.: Role of nitrite in the photochemical formation of radicals in the snow, Environ. Sci. Technol., 48(1), 165–172, doi:10.1021/es404002c, 2014.

Kahl, J. D. W., Martinez, D. A., Kuhns, H., Davidson, C. I., Jafferezo, J. L. and Harris, J. M.: Air mass trajectories to Summit, Greenland : A 44-year climatology and some episodic events, J. Geophys. Res. Ocean., 102(C12), 26861–26875, 1997.

Kerkweg, A., Jöckel, P., Warwick, N., Gebhardt, S., Brenninkmeijer, C. a. M. and Lelieveld, J.: Consistent simulation of bromine chemistry from the marine boundary layer to the stratosphere – Part 2 : Bromocarbons, Atmos. Chem. Phys. Discuss., 8(3), 9477–9530, doi:10.5194/acpd-8-9477-2008,

538 2008.

539 Kinnard, C., Zdanowicz, C. M., Koerner, R. M. and Fisher, D. A.: A changing Arctic seasonal ice zone:
540 Observations from 1870-2003 and possible oceanographic consequences, Geophys. Res. Lett., 35(2),
541 2–6, doi:10.1029/2007GL032507, 2008.

542 Lamarque, J.-F., Dentener, F., McConnell, J., Ro, C.-U., Shaw, M., Vet, R., Bergmann, D., Cameron-
543 Smith, P., Dalsoren, S., Doherty, R., Faluvegi, G., Ghan, S. J., Josse, B., Lee, Y. H., MacKenzie, I. A.,
544 Plummer, D., Shindell, D. T., Skeie, R. B., Stevenson, D. S., Strode, S., Zeng, G., Curran, M., Dahl-
545 Jensen, D., Das, S., Fritzsche, D. and Nolan, M.: Multi-model mean nitrogen and sulfur deposition from
546 the Atmospheric Chemistry and Climate Model Intercomparison Project (ACCMIP): evaluation of
547 historical and projected future changes, Atmos. Chem. Phys., 13(16), 7997–8018, doi:10.5194/acp-13-
548 7997-2013, 2013.

549 Langendörfer, U., Lehrer, E., Wagenbach, D. and Platt, U.: Observation of filterable bromine
550 variabilities during Arctic tropospheric ozone depletion events in high (1 hour) time resolution, in
551 Journal of Atmospheric Chemistry, vol. 34, pp. 39–54., 1999.

552 Legrand, M., Hammer, C., De Angelis, M., Savarino, J., Delmas, R., Clausen, H. and Johnsen, S. J.:
553 Sulfur-containing species (methanesulfonate and SO4) over the last climatic cycle in the Greenland Ice
554 Core Project (central Greenland) ice core, J. Geophys. Res., 102(C12), 26663, doi:10.1029/97JC01436,
555 1997.

556 Lehrer, E., Wagenbach, D. and Platt, U.: Aerosol chemical composition during tropospheric ozone
557 depletion at Ny Ålesund/Svalbard, Tellus B, 49(5), doi:10.3402/tellusb.v49i5.15987, 1997.

558 Li, S.-M. and Barrie, L. A.: Biogenic sulfur aerosol in the Arctic troposphere: 1. Contributions to total
559 sulfate, J. Geophys. Res., 98(D11), 20613, doi:10.1029/93JD02234, 1993.

560 Macias Fauria, M., Grinsted, A., Helama, S., Moore, J., Timonen, M., Martma, T., Isaksson, E. and
561 Eronen, M.: Unprecedented low twentieth century winter sea ice extent in the Western Nordic Seas
562 since A.D. 1200, Clim. Dyn., 34(6), 781–795, doi:10.1007/s00382-009-0610-z, 2010.

563 Mann, M. E., Bradley, R. S. and Hughes, M. K.: Global-scale temperature patterns and climate forcing
564 over the past six centuries, Nature, 392(6678), 779–787, doi:10.1038/33859, 1998.

565 McConnell, J. R. and Edwards, R.: Coal burning leaves toxic heavy metal legacy in the Arctic., Proc.
566 Natl. Acad. Sci. U. S. A., 105(34), 12140–12144, doi:10.1073/pnas.0803564105, 2008.

567 McConnell, J. R., Lamorey, G. W., Lambert, S. W. and Taylor, K. C.: Continuous ice-core chemical
568 analyses using inductively coupled plasma mass spectrometry., Environ. Sci. Technol., 36(775), 7–11,

569 doi:10.1021/es011088z, 2002.

570 McConnell, J. R., Edwards, R., Kok, G. L., Flanner, M. G., Zender, C. S., Saltzman, E. S., Banta, J. R.,
571 Pasteris, D. R., Carter, M. M. and Kahl, J. D. W.: 20th-Century Industrial Black Carbon Emissions
572 Altered Arctic Climate Forcing, Science (80-.)., 317(5843), 1381–1384, doi:10.1126/science.1144856,
573 2007.

574 Millero, F. J.: The Physical Chemistry of Seawater, Annu. Rev. Earth Planet. Sci., 2(1), 101–150,
575 doi:10.1146/annurev.ea.02.050174.000533, 1974.

576 Moldanová, J. and Ljungström, E.: Sea-salt aerosol chemistry in coastal areas: A model study, J.
577 Geophys. Res., 106, 1271, doi:10.1029/2000JD900462, 2001.

578 Montzka, S. and Reimann, S.: Scientific Assessment of Ozone Depletion 2010: Scientific Summary
579 Chapter 1 Ozone-Depleting Substances (ODSs) and Related Chemicals. [online] Available from:
580 http://www.esrl.noaa.gov/csd/assessments/ozone/2010/summary/ch1.html (Accessed 23 December
581 2015), 2010.

582 Morin, S., Savarino, J., Frey, M. M., Yan, N., Bekki, S., Bottenheim, J. and Martins, J. M. F.: Tracing
583 the origin and fate of NOx in the Arctic atmosphere using stable isotopes in nitrate., Science, 322(5902),
584 730–2, doi:10.1126/science.1161910, 2008.

585 Mulvaney, R., Pasteur, E. C., Peel, D. A., Saltzman, E. S. and Whung, P.-Y.: The ratio of MSA to non-
586 sea-salt sulphate in Antarctic Peninsula ice cores, Tellus B, 44(4), doi:10.3402/tellusb.v44i4.15457,
587 1992.

588 Nghiem, S. V., Rigor, I. G., Richter, A., Burrows, J. P., Shepson, P. B., Bottenheim, J., Barber, D. G.,
589 Steffen, A., Latonas, J., Wang, F., Stern, G., Clemente-Colón, P., Martin, S., Hall, D. K., Kaleschke, L.,
590 Tackett, P., Neumann, G. and Asplin, M. G.: Field and satellite observations of the formation and
591 distribution of Arctic atmospheric bromine above a rejuvenated sea ice cover, J. Geophys. Res. Atmos.,
592 117(D17), n/a–n/a, doi:10.1029/2011JD016268, 2012.

593 O'Dwyer, J., Isaksson, E., Vinje, T., Jauhiainen, T., Moore, J., Pohjola, V., Vaikmae, R. and van de
594 Wal, R. S. W.: Methanesulfonic acid in a Svalbard ice core as an indicator of ocean climate, Geophys.
595 Res. Lett., 27(8), 1159–1162, doi:10.1029/1999GL011106, 2000.

596 Ordóñez, C., Lamarque, J.-F., Tilmes, S., Kinnison, D. E., Atlas, E. L., Blake, D. R., Sousa Santos, G.,
597 Brasseur, G. and Saiz-Lopez, A.: Bromine and iodine chemistry in a global chemistry-climate model:
598 description and evaluation of very short-lived oceanic sources, Atmos. Chem. Phys., 12(3), 1423–1447,
599 doi:10.5194/acp-12-1423-2012, 2012.

700 Parrella, J. P., Jacob, D. J., Liang, Q., Zhang, Y., Mickley, L. J., Miller, B., Evans, M. J., Yang, X., Pyle,
701 J. A., Theys, N. and Van Roozendael, M.: Tropospheric bromine chemistry: implications for present
702 and pre-industrial ozone and mercury, Atmos. Chem. Phys., 12(15), 6723–6740, doi:10.5194/acp-12-
703 6723-2012, 2012.

704 Pasteris, D. R., McConnell, J. R. and Edwards, R.: High-resolution, continuous method for measurement
705 of acidity in ice cores, Environ. Sci. Technol., 46, 1659–1666, doi:10.1021/es202668n, 2012.

706 Pratt, K. A., Custard, K. D., Shepson, P. B., Douglas, T. A., Pöhler, D., General, S., Zielcke, J., Simpson,
707 W. R., Platt, U., Tanner, D. J., Gregory Huey, L., Carlsen, M. and Stirm, B. H.: Photochemical
708 production of molecular bromine in Arctic surface snowpacks, Nat. Geosci., 6(5), 351–356,
709 doi:10.1038/ngeo1779, 2013.

710 Rankin, A. M., Wolff, E. W. and Martin, S.: Frost flowers: Implications for tropospheric chemistry and
711 ice core interpretation, J. Geophys. Res. Atmos., 107(D23), 4683, doi:10.1029/2002JD002492, 2002.

712 Rayner, N. A.: Global analyses of sea surface temperature, sea ice, and night marine air temperature
713 since the late nineteenth century, J. Geophys. Res., 108(D14), 4407, doi:10.1029/2002JD002670, 2003.

714 Röthlisberger, R., Bigler, M., Hutterli, M., Sommer, S., Stauffer, B., Junghans, H. G. and Wagenbach,
715 D.: Technique for continuous high-resolution analysis of trace substances in firn and ice cores, Environ.
716 Sci. Technol., 34(2), 338–342, doi:10.1021/es9907055, 2000.

717 Röthlisberger, R., Mulvaney, R., Wolff, E. W., Hutterli, M. a., Bigler, M., Sommer, S. and Jouzel, J.:
718 Dust and sea salt variability in central East Antarctica (Dome C) over the last 45 kyrs and its implications
719 for southern high-latitude climate, Geophys. Res. Lett., 29(20), 1–4, doi:10.1029/2003GL016936, 2002.

720 Saltzman, E. S., Dioumaeva, I. and Finley, B. D.: Glacial/interglacial variations in methanesulfonate
721 (MSA) in the Siple Dome ice core, West Antarctica, Geophys. Res. Lett., 33(11), 1–4,
722 doi:10.1029/2005GL025629, 2006.

723 Sander, R., Rudich, Y., von Glasow, R. and Crutzen, P. J.: The role of BrNO3 in marine tropospheric
724 chemistry: A model study, Geophys. Res. Lett., 26(18), 2857–2860, doi:10.1029/1999GL900478, 1999.

725 Sander, R., Keene, W. C., Pszenny, a. a. P., Arimoto, R., Ayers, G. P., Baboukas, E., Cainey, J. M.,
726 Crutzen, P. J., Duce, R. a., Hönninger, G., Huebert, B. J., Maenhaut, W., Mihalopoulos, N., Turekian,
727 V. C. and Van Dingenen, R.: Inorganic bromine in the marine boundary layer: a critical review, Atmos.
728 Chem. Phys. Discuss., 3, 1301–1336, doi:10.5194/acpd-3-2963-2003, 2003.

729 Schönhardt, A., Begoin, M., Richter, A., Wittrock, F., Kaleschke, L., Gómez Martín, J. C. and Burrows,
730 J. P.: Simultaneous satellite observations of IO and BrO over Antarctica, Atmos. Chem. Phys., 12(14),

731 6565–6580, doi:10.5194/acp-12-6565-2012, 2012.

732 Sharma, S., Chan, E., Ishizawa, M., Toom-Sauntry, D., Gong, S. L., Li, S. M., Tarasick, D. W., Leaitch,
733 W. R., Norman, a., Quinn, P. K., Bates, T. S., Levasseur, M., Barrie, L. a. and Maenhaut, W.: Influence
734 of transport and ocean ice extent on biogenic aerosol sulfur in the Arctic atmosphere, J. Geophys. Res.
735 Atmos., 117(12), n/a–n/a, doi:10.1029/2011JD017074, 2012.

736 Sigl, M., McConnell, J. R., Layman, L., Maselli, O. J., McGwire, K., Pasteris, D., Dahl-Jensen, D.,
737 Steffensen, J. P., Vinther, B., Edwards, R., Mulvaney, R. and Kipfstuhl, S.: A new bipolar ice core
738 record of volcanism from WAIS Divide and NEEM and implications for climate forcing of the last 2000
739 years, J. Geophys. Res. Atmos., 118(3), 1151–1169, doi:10.1029/2012JD018603, 2013.

740 Sigl, M., Winstrup, M., McConnell, J. R., Welten, K. C., Plunkett, G., Ludlow, F., Büntgen, U., Caffee,
741 M., Chellman, N., Dahl-Jensen, D., Fischer, H., Kipfstuhl, S., Kostick, C., Maselli, O. J., Mekhaldi, F.,
742 Mulvaney, R., Muscheler, R., Pasteris, D. R., Pilcher, J. R., Salzer, M., Schüpbach, S., Steffensen, J. P.,
743 Vinther, B. M. and Woodruff, T. E.: Timing and climate forcing of volcanic eruptions for the past 2,500
744 years, Nature, 523(7562), 543–9, doi:10.1038/nature14565, 2015.

745 Simpson, W. R., von Glasow, R., Riedel, K., Anderson, P., Ariya, P., Bottenheim, J., Burrows, J.,
746 Carpenter, L. J., Friess, U., Goodsite, M. E., Heard, D., Hutterli, M., Jacobi, H.-W., Kaleschke, L., Neff,
747 B., Plane, J., Platt, U., Richter, a., Roscoe, H., Sander, R., Shepson, P., Sodeau, J., Steffen, a., Wagner,
748 T. and Wolff, E.: Halogens and their role in polar boundary-layer ozone depletion, , 4375–4418,
749 doi:10.5194/acpd-7-4285-2007, 2007.

750 Sjostedt, S. J., Huey, L. G., Tanner, D. J., Peischl, J., Chen, G., Dibb, J. E., Lefer, B., Hutterli, M. a.,
751 Beyersdorf, a. J., Blake, N. J., Blake, D. R., Sueper, D., Ryerson, T., Burkhart, J. and Stohl, a.:
752 Observations of hydroxyl and the sum of peroxy radicals at Summit, Greenland during summer 2003,
753 Atmos. Environ., 41(24), 5122–5137, doi:10.1016/j.atmosenv.2006.06.065, 2007.

754 Smith, S. J., van Aardenne, J., Klimont, Z., Andres, R. J., Volke, A. and Delgado Arias, S.:
755 Anthropogenic sulfur dioxide emissions: 1850–2005, Atmos. Chem. Phys., 11(3), 1101–1116,
756 doi:10.5194/acp-11-1101-2011, 2011.

757 Spolaor, A., Vallelonga, P., Plane, J. M. C., Kehrwald, N., Gabrieli, J., Varin, C., Turetta, C., Cozzi, G.,
758 Kumar, R., Boutron, C. and Barbante, C.: Halogen species record Antarctic sea ice extent over glacial-
759 interglacial periods, Atmos. Chem. Phys., 13, 6623–6635, doi:10.5194/acp-13-6623-2013, 2013a.

760 Spolaor, A., Gabrieli, J., Martma, T., Kohler, J., Björkman, M. B., Isaksson, E., Varin, C., Vallelonga,
761 P., Plane, J. M. C. and Barbante, C.: Sea ice dynamics influence halogen deposition to Svalbard,
762 Cryosph., 7(5), 1645–1658, doi:10.5194/tc-7-1645-2013, 2013b.

763 Spolaor, A., Vallelonga, P., Gabrieli, J., Martma, T., Björkman, M. P., Isaksson, E., Cozzi, G., Turetta,
764 C., Kjær, H. A., Curran, M. A. J., Moy, A. D., Schönhardt, A., Blechschmidt, A.-M., Burrows, J. P.,
765 Plane, J. M. C. and Barbante, C.: Seasonality of halogen deposition in polar snow and ice, Atmos. Chem.
766 Phys., 14(18), 9613–9622, doi:10.5194/acp-14-9613-2014, 2014.

767 Spolaor, A., Opel, T., McConnell, J. R., Maselli, O. J., Spreen, G., Varin, C., Kirchgeorg, T., Fritzsche,
768 D., Saiz-Lopez, A. and Vallelonga, P.: Halogen-based reconstruction of Russian Arctic sea ice area
769 from the Akademii Nauk ice core (Severnaya Zemlya), Cryosph., 10, 245–256, doi:10.5194/tcd-9-4407-
770 2015, 2016.

771 Sturges, W. T. and Harrison, R. M.: Bromine:Lead ratios in airborne particles from urban and rural sites,
772 Atmos. Environ., 20(3), 577–588, doi:10.1016/0004-6981(86)90101-0, 1986.

773 Thomas, V. M., Bedford, J. A. and Cicerone, R. J.: Bromine emissions from leaded gasoline, Geophys.
774 Res. Lett., 24(11), 1371–1374, doi:10.1029/97GL01243, 1997.

775 Vestreng, V., Ntziachristos, L., Semb, A., Reis, S., Isaksen, I. S. A. and Tarrasón, L.: Evolution of NO_x
776 emissions in Europe with focus on road transport control measures, Atmos. Chem. Phys., 9(4), 1503–
777 1520, doi:10.5194/acp-9-1503-2009, 2009.

778 Wagner, T., Leue, C., Wenig, M., Pfeilsticker, K. and Platt, U.: Spatial and temporal distribution of
779 enhanced boundary layer BrO concentrations measured by the GOME instrument aboard ERS-2, J.
780 Geophys. Res., 106(D20), 24225, doi:10.1029/2000JD000201, 2001.

781 Walsh, J. E.: A data set on Northern Hemisphere sea ice extent, Natl. Snow Ice Data Cent., 49–51, 1978.

782 Weißbach, S., Wegner, A., Opel, T., Oerter, H., Vinther, B. M. and Kipfstuhl, S.: Spatial and temporal
783 oxygen isotope variability in northern Greenland - implications for a new climate record over the past
784 millennium, Clim. Past Discuss., 11(3), 2341–2388, doi:10.5194/cpd-11-2341-2015, 2015.

785 Weller, R.: Postdepositional losses of methane sulfonate, nitrate, and chloride at the European Project
786 for Ice Coring in Antarctica deep-drilling site in Dronning Maud Land, Antarctica, J. Geophys. Res.,
787 109(D7), 1–9, doi:10.1029/2003JD004189, 2004.

788 WMO: Scientific Assessment of Ozone Depletion: 1994. Chapter 10: Methyl Bromide, Geneva., 1995.

789 WMO: Scientific Assessment of Ozone Depletion: 2002. Chapter 1: Controlled Substances and Other
790 Source Gases., 2002.

791 Wolff, E. W.: Ice sheets and nitrogen, Philos. Trans. R. Soc. Lond. B. Biol. Sci., 368,
792 doi:10.1098/rstb.2013.0127, 2013.

793 Wolff, E. W., Rankin, A. M. and Röthlisberger, R.: An ice core indicator of Antarctic sea ice

794 production?, Geophys. Res. Lett., 30(22), 2–5, doi:10.1029/2003GL018454, 2003.

795 Xu, L., Russell, L. M., Somerville, R. C. J. and Quinn, P. K.: Frost flower aerosol effects on Arctic
796 wintertime longwave cloud radiative forcing, J. Geophys. Res. Atmos., 118(23), 13282–13291,
797 doi:10.1002/2013JD020554, 2013.

798 Yang, X., Pyle, J. A. and Cox, R. A.: Sea salt aerosol production and bromine release: Role of snow on
799 sea ice, Geophys. Res. Lett., 35(16), 1–5, doi:10.1029/2008GL034536, 2008.

800 Yang, X., Pyle, J. A., Cox, R. A., Theys, N. and Van Roozendael, M.: Snow-sourced bromine and its
801 implications for polar tropospheric ozone, Atmos. Chem. Phys., 10(16), 7763–7773, doi:10.5194/acp-
802 10-7763-2010, 2010.

803 Yung, Y. L., Pinto, J. P., Watson, R. T. and Sander, S. P.: Atmospheric Bromine and Ozone
804 Perturbations in the Lower Stratosphere, J. Atmos. Sci., 37(2), 339–353, doi:10.1175/1520-
805 0469(1980)037<0339:ABAOPI>2.0.CO;2, 1980.

806

807

808

809

Clim. Past Discuss., doi:10.5194/cp-2016-49, 2016
Manuscript under review for journal Clim. Past
Published: 10 May 2016

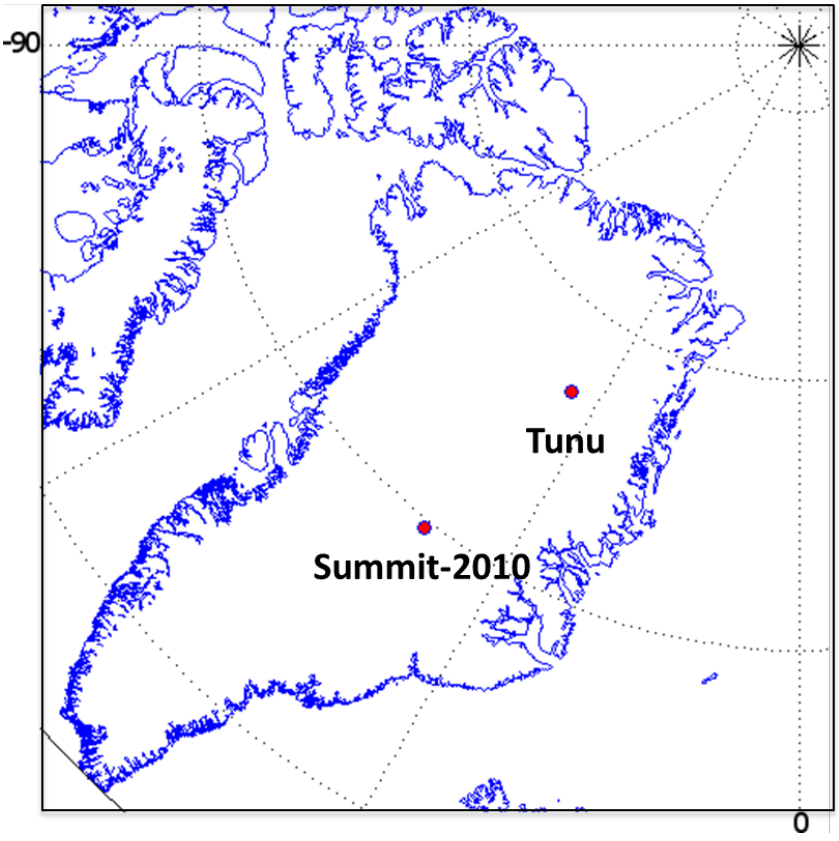

310

311 **Figure 1.** Locations of ice cores used in this study. Summit-2010: (72°20'N 38°17'24"W), Tunu: (78°
312 2' 5.5"N, 33° 52' 48"W)

313

314

315

316

317

318

Clim. Past Discuss., doi:10.5194/cp-2016-49, 2016
Manuscript under review for journal Clim. Past
Published: 10 May 2016

Climate of the Past
Discussions
Open Access
EGU

319

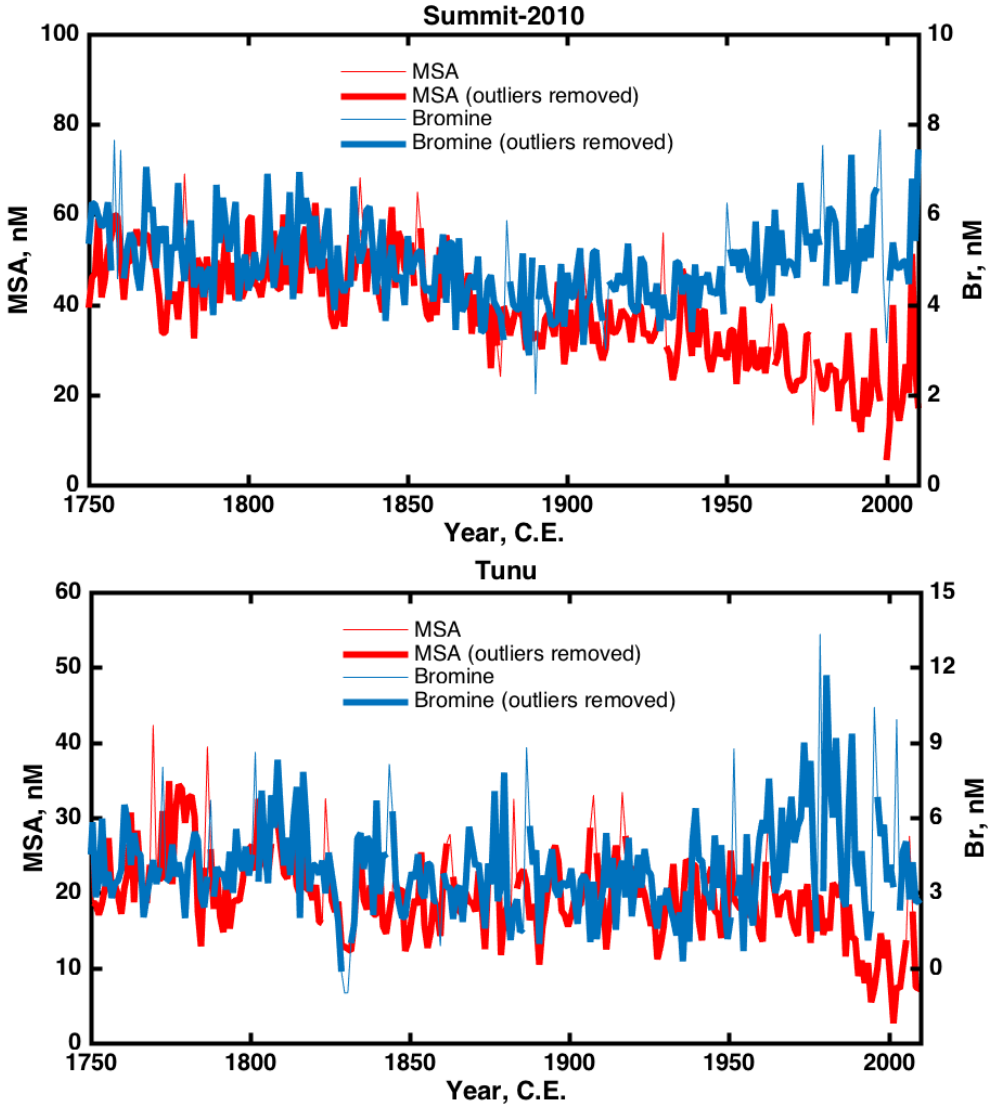

320

321

322 **Figure 2.** Annual record of bromine (thin blue) and MSA (thin red). Annual record of bromine (thick
323 blue) and MSA (thick red) with outlying spikes removed using a 25 year running average filter described
324 by Sigl et al. (2013). All records were fit with a 3 step linear regression and the results of the fits which
325 identify the timing of inflection points are summarized in Table S1.

Clim. Past Discuss., doi:10.5194/cp-2016-49, 2016
Manuscript under review for journal Clim. Past
Published: 10 May 2016

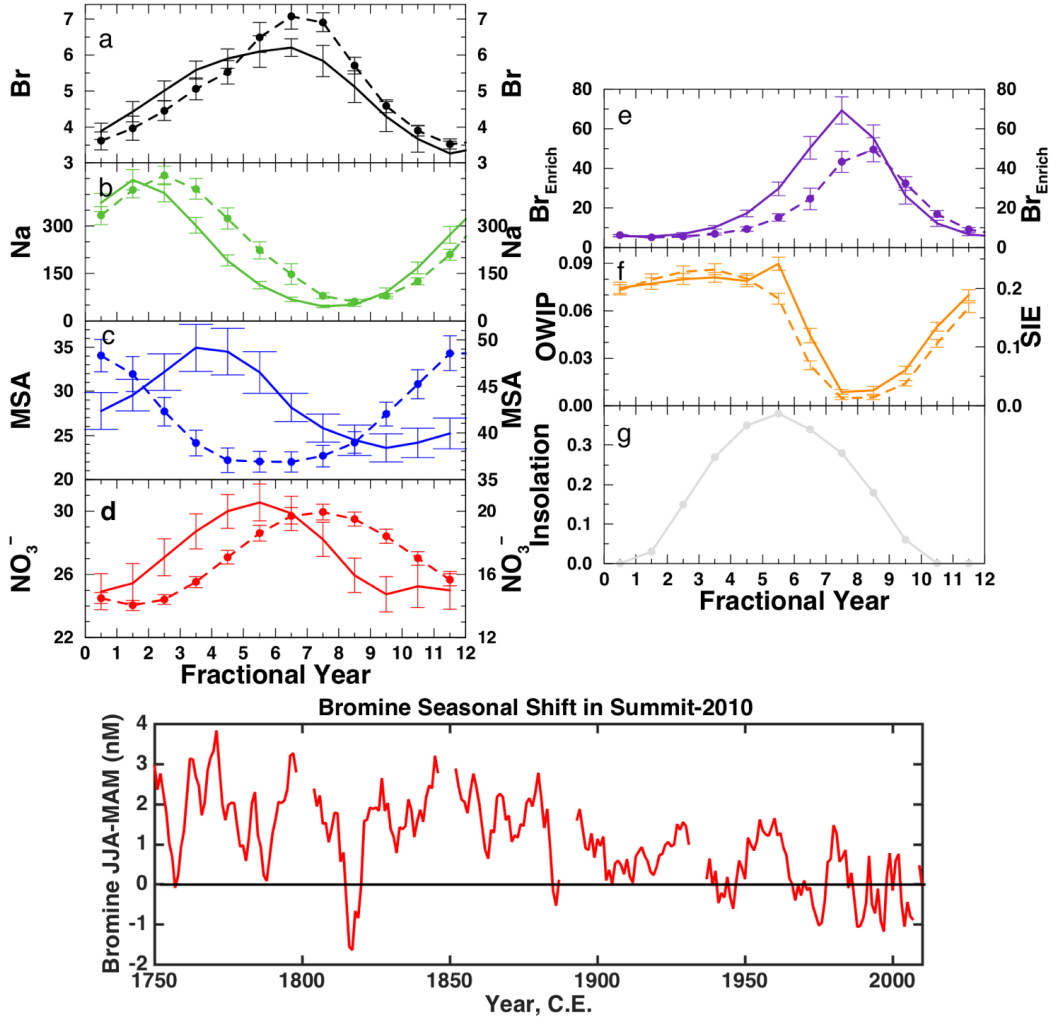

Figure 3. Upper plots: Average seasonal cycle of species in the Summit-2010 ice core. The left-hand Y axes are associated with the solid lines, and the right-hand Y axes associated with the dashed lines. Dashed lines (a-e): Average seasonal cycle from depths 43.5 – 87.3 m (years 1742-1900). Solid lines (a-e): Average seasonal cycle from 0-43.5 m (years 1900-2010). Error bars indicate the standard error of the monthly value. (a) Total bromine, (b) total sodium, (c) MSA, (d) nitrate. Units for (a-d) are nM. Note that the seasonal cycle in bromine appears to broaden in the 1900-2010 period (see lower panel). Note also that the MSA maximum shifts from spring in the shallowest part of the ice core (solid line) to winter in the deepest part of the ice core (dashed line) due to post-depositional effects (see Fig. S3). (e) Average seasonal cycle in bromine enrichment (relative to sea salt sodium, see Eq. (4)). (f-right) The sea ice extent (SIE) within an area of the East Greenland coast [70°− 63° N, 15°− 45° W] that shows

Clim. Past Discuss., doi:10.5194/cp-2016-49, 2016
Manuscript under review for journal Clim. Past
Published: 10 May 2016

337 highest correlations to MSA (see Fig. 6), (f – left) Area of open water within the sea ice pack (OWIP)
338 for the area defined by SIE. (g) Solar insolation at 12 GMT at the latitude of Summit
339 (eosweb.larc.nasa.gov). Lower plot: Broadening of bromine seasonal cycle in the Summit-2010 ice core.
340 The difference between the summer and spring bromine signal (JJA-MAM) was monitored over the
341 length of the entire ice core. In the preindustrial era (pre-1850) bromine peaks in summer; realised as
342 positive values of JJA-MAM. After 1900 there is a marked broadening of the seasonal signal towards
343 spring and by ~1970 the seasonal signal maximum is routinely shared between summer and spring
344 realised as an averaged JJA-MAM of approximately zero.
345

Clim. Past Discuss., doi:10.5194/cp-2016-49, 2016
Manuscript under review for journal Clim. Past
Published: 10 May 2016

Climate of the Past Discussions
Open Access
EGU

346

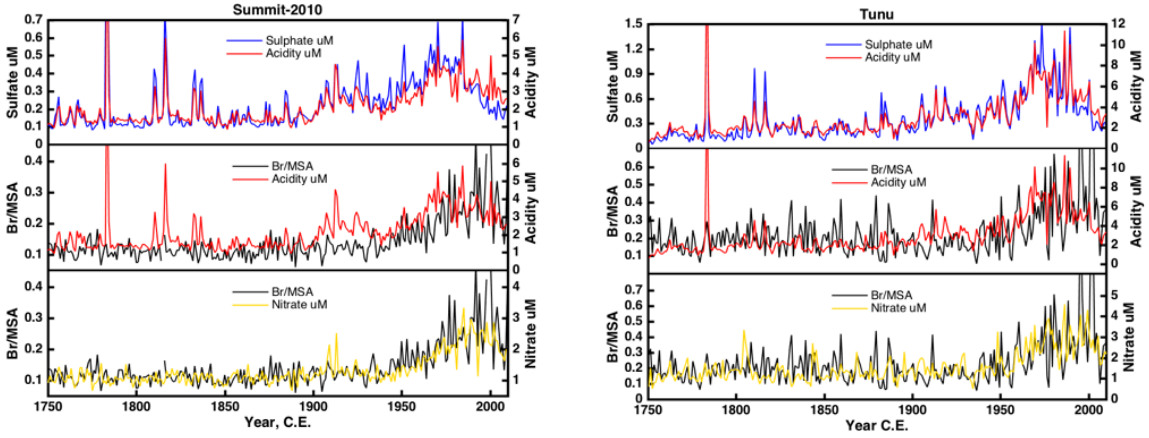

347

348 **Figure 4.** Comparison between the measured total sulfur (shown as sulfate) and acidity records from
349 each ice core (top panels). The acidity record is dominated by the influence of the sulfur species until
350 the early 21th century when the NOx pollution remains elevated whilst anthropogenic sulfur sources are
351 depleted resulting in a slight relative elevation of the total acidity relative to total sulfur concentrations.
352 The large spikes in the acidity and sulfur records are identified as volcanic events. The ice core records
353 cover the period of the 1783 Laki eruption as well as the Unknown 1909 eruption and Tambora eruption
354 (Indonesia) in 1815 (Sigl et al., 2013). Comparison between Br/MSA and total acidity (center panels)
355 and nitrate (NO_3^-, bottom panels) measured in the ice cores. The Br/MSA ratio follows the total acidity
356 record closely except where the record is dominated by the sulphur component (e.g. early 1900s). Of
357 the two major acidic species the Br/MSA follows the nitrate most closely at both ice core sites.

358

359

360

361

Clim. Past Discuss., doi:10.5194/cp-2016-49, 2016
Manuscript under review for journal Clim. Past
Published: 10 May 2016

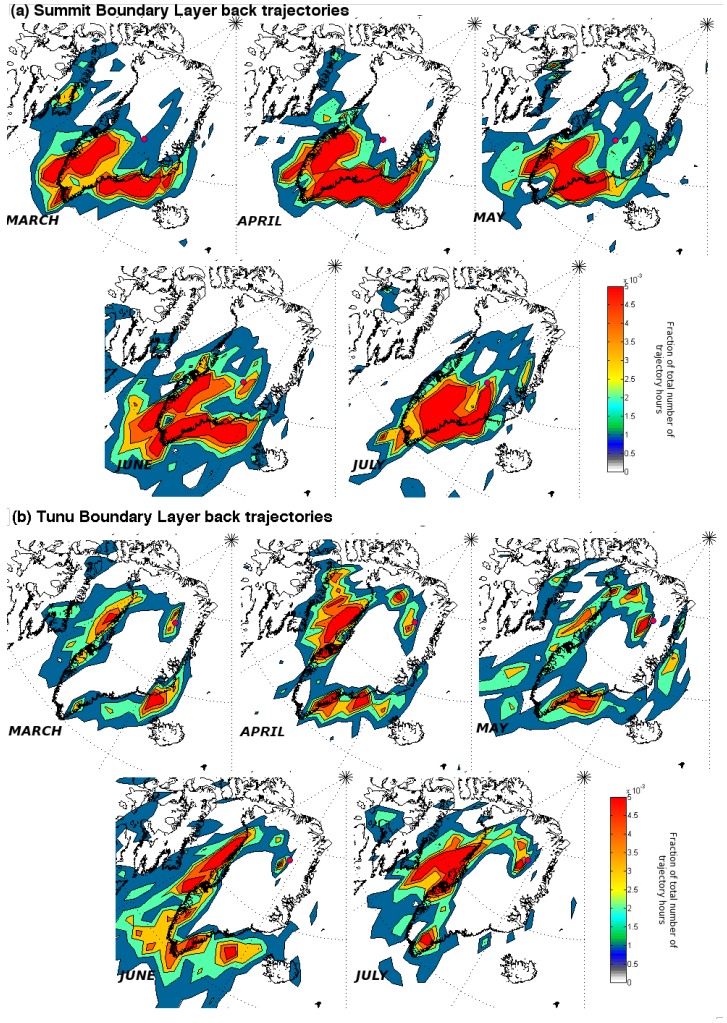

Figure 5. Air mass back trajectories from the (a) Summit-2010 and (b) Tunu ice core sites over the period 2005-2013 C.E. Maps display the fraction of the total number of trajectory hours (ranging between 21400-25500 hr month^{-1}) spent at altitudes under 500 m. Back trajectories were allowed to travel for 10 hr. New trajectories were started every 12 hours. Map grid resolution is 2°x 2°. Ice core locations are shown by a pink circle. Maps show that air masses consistently arrive at Summit from the SE Greenland coast with a smaller contribution from the SW coast. Air masses consistently arrive at Tunu from the western Greenland coast with a smaller contribution from the SE and NE coast. The air mass originating from the NE coast is most dominant in May and comparison with the total vertical column profile (Fig. S4) shows it is confined to lower altitudes unlike those from the west coast.

Clim. Past Discuss., doi:10.5194/cp-2016-49, 2016
Manuscript under review for journal Clim. Past
Published: 10 May 2016

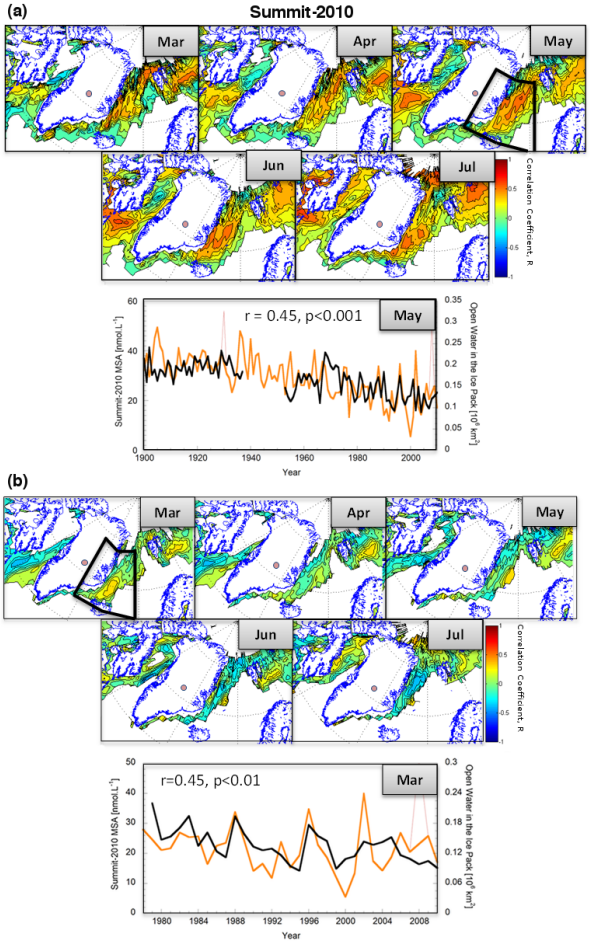

Figure 6. Correlation maps of monthly sea ice concentration (SIC) derived from the Summit-2010 ice core. (a) HadISST1 ICE dataset from 1900-2012 C.E. correlated with annual records of MSA. Outliers were removed from the MSA records before the correlations were performed. Month labels indicate month of SIC compared with the annual MSA value. Only locations that showed a SIC variability greater than 10% and have a significant correlation (t-test, $p<0.05$) are displayed. The area of sea ice that is the likely source of MSA (as indicated by the air-mass trajectories) are outlined in black [70°– 63° N, 15°– 45° W]. Graphed is the area of open water in the sea ice in this region (OWIP, black) overlaid on the annual MSA record (red, outliers removed - orange). (b) As for the upper panel but focused on the satellite period 1979-2012 C.E. Summit MSA shows a significant, positive correlation with the amount of OWIP during spring within the integrated region.

Clim. Past Discuss., doi:10.5194/cp-2016-49, 2016
Manuscript under review for journal Clim. Past
Published: 10 May 2016

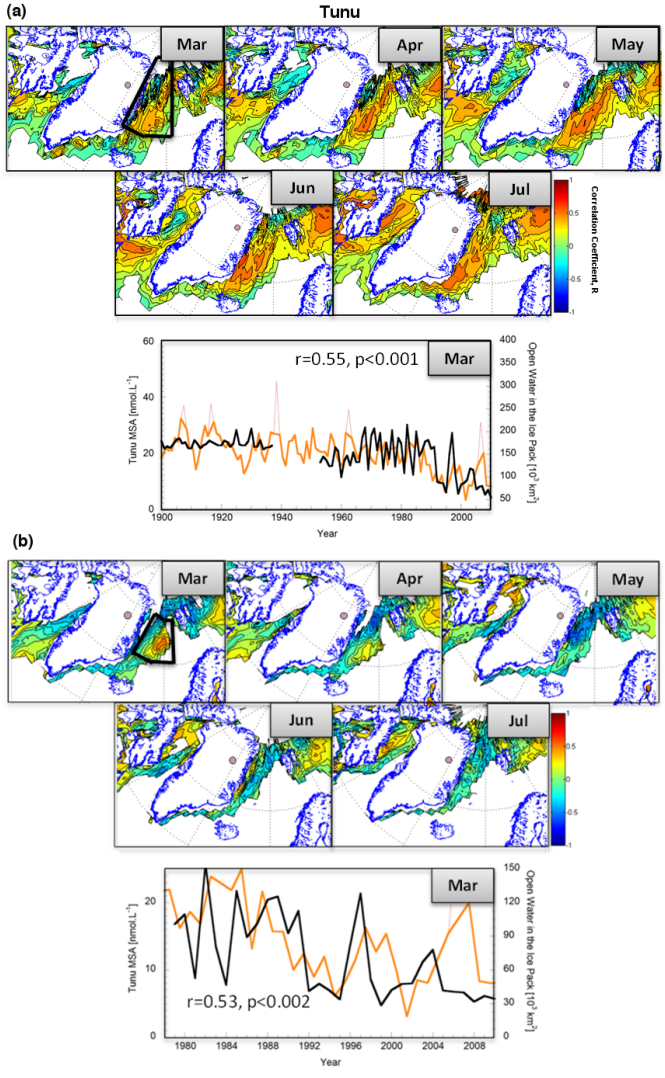

Figure 7. Correlation maps of monthly sea ice concentration (SIC) derived from the Tunu ice core. (a) HadISST1 ICE dataset from 1900-2012 C.E. correlated with annual records of MSA. Outliers were removed from the MSA records before the correlations were performed. Month labels indicate the month of SIC compared with the annual MSA value. Only locations that showed a SIC variability greater than 10% and have a significant correlation (t-test, $p<0.05$) are displayed. The area of sea ice that is the likely source of MSA (as indicated by the air-mass trajectories) are outlined in black [80°– 73° N, 20°– 0° W]. Graphed is the area of open water in the sea ice in this region (OWIP, black) overlaid on the annual MSA record (red, outliers removed - orange). Like in the Summit-20101 ice core, Tunu

Clim. Past Discuss., doi:10.5194/cp-2016-49, 2016
Manuscript under review for journal Clim. Past
Published: 10 May 2016

392 MSA also shows a significant, positive correlation with the amount of OWIP during spring but the
393 correlation is highest when MSA is compared to the annual OWIP in the source region. (b) As for the
394 upper panel but focused on the satellite period 1979-2012 C.E. Again MSA shows a significant, positive
395 correlation with the amount of OWIP during spring at both sites. During the satellite period the
396 correlation between OWIP and MSA concentrations at Tunu is greatly increased when a second, closer
397 region is also included in the integration [80°−73° N, 20° −0° W].
398

Clim. Past Discuss., doi:10.5194/cp-2016-49, 2016
Manuscript under review for journal Clim. Past
Published: 10 May 2016

Climate of the Past Discussions
Open Access
EGU

399

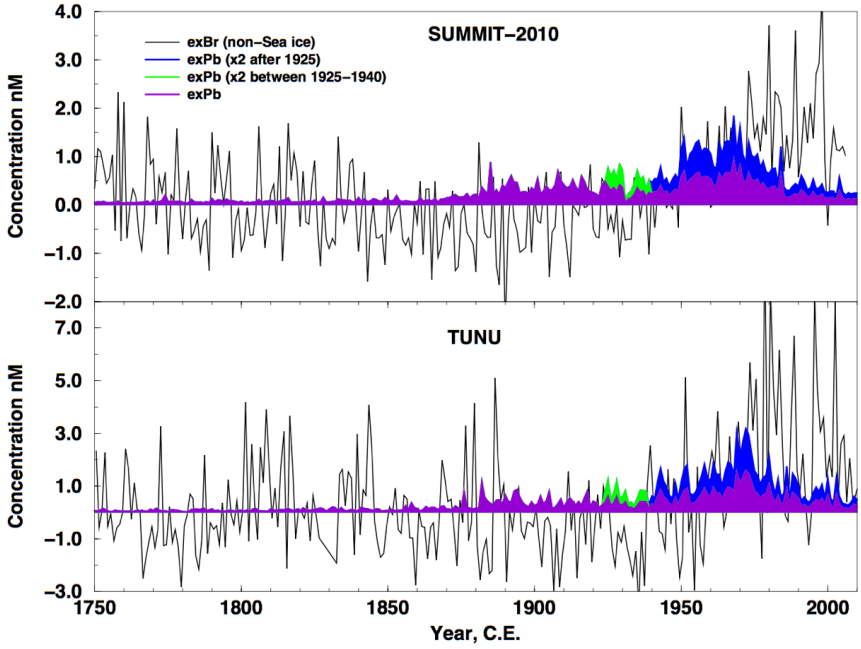

400

401 **Figure 8.** Comparison between measurements of excess lead (exPb, purple shading) and bromine in
402 excess of what is expected from the preindustrial (1750-1880) Br/MSA relationship (exBr, black).
403 Between 1925-1940 world-wide leaded gasoline sources contained a Pb:Br molar ratio of 1:2 (aviation
404 fuel). After 1940 only Russia continued to use the 1:2 ratio in their leaded fuel whilst the rest of the
405 world changed to a 1:1 ratio. The green shading shows an estimate of bromine from leaded fuel
406 combustion over the 1925-1940 period (relative to the exPb concentrations). The blue shading shows
407 the upper limit to the amount of bromine (relative to exPb) that could be derived from leaded fuel
408 combustion by assuming Pb:Br ratio of 1:2 after 1940. After 1970, when world consumption of leaded
409 gasoline began to fall, exBr concentrations continued to rise at both ice core sites far above the
410 concentrations that could be explained by leaded gasoline sources.

411

412

413

Clim. Past Discuss., doi:10.5194/cp-2016-49, 2016
Manuscript under review for journal Clim. Past
Published: 10 May 2016

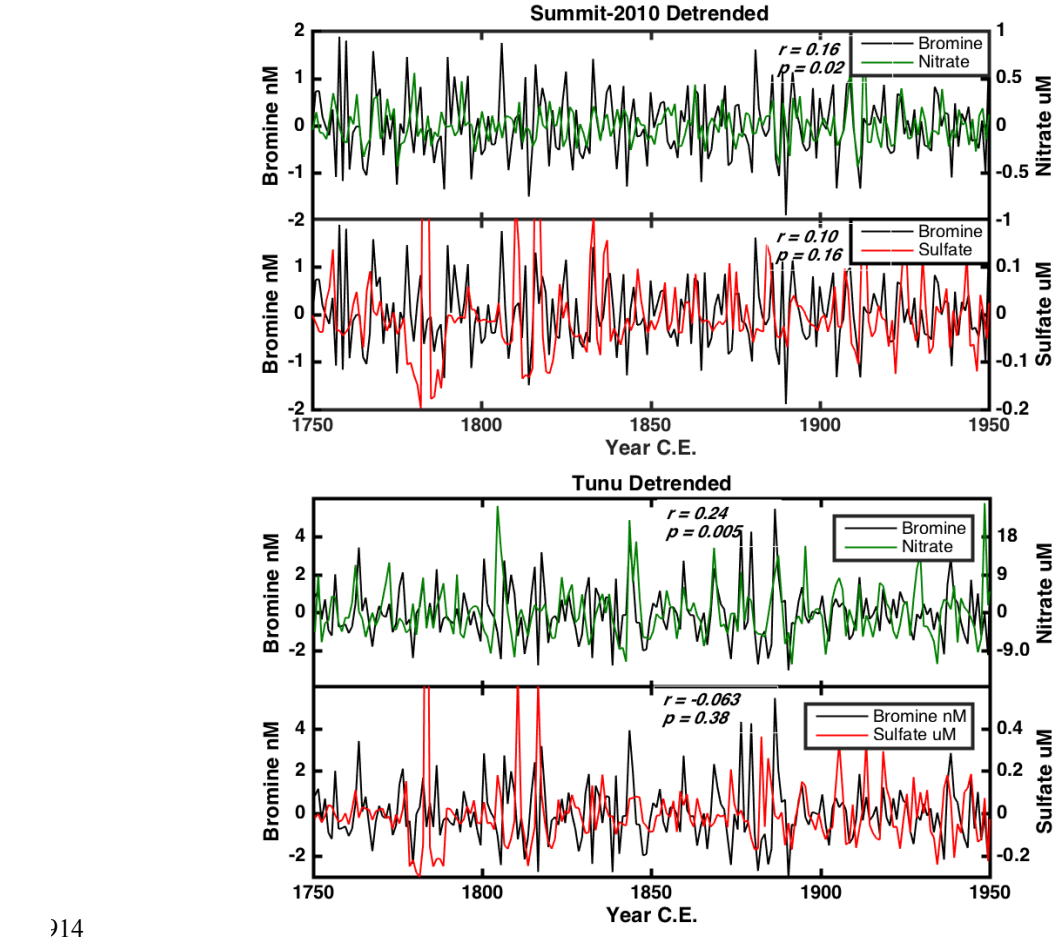

Figure 9. High frequency comparison between the annual bromine, nitrate and sulfate records measured in the ice cores. Each series has been detrended with an 11 year running average before comparison to remove the low frequency changes in each record. The correlation is highest between bromine and nitrate at both sites. The r-value for bromine versus nitrate at Summit increases in significance (r= 0.24,p=0.001) when the entire period (1750-2010) is considered. At both sites there is a close relationship between the variability in the nitrate and bromine due to their intimate relationship during emission from the sea ice, transport and deposition onto the snow pack. The correlation between sulfate (or indeed bulk acidity) and bromine is not significant significant over any of the time periods shown at either site. Particularly evident is the non-response of the bromine signal to the sulfur rich volcanic events as described in Sect.4.2.2.